

# Spatio-stochastic adaptive discontinuous Galerkin methods

Geoff Donoghue<sup>a,\*</sup>, Masayuki Yano<sup>a</sup>

<sup>a</sup>University of Toronto, 4925 Dufferin Street, Toronto, Ontario, M5H 5T6, Canada

---

## Abstract

We introduce a goal-oriented, adaptive framework for the uncertainty quantification of systems modeled by stochastically parametrized nonlinear hyperbolic and convection-dominated partial differential equations. Of particular interest are conservation laws in aerodynamics that may have a small number of stochastic parameters but exhibit strong nonlinearity and a wide range of scales. Our framework exploits localized structure in the spatio-parameter space to enable rapid, reliable uncertainty quantification for output quantities of interest. Our formulation comprises the following technical components: (i) a discontinuous Galerkin finite element method, which provides stability for convection-dominated problems; (ii) element-wise polynomial chaos expansions, which capture the parametric dependence of the solution in a way amenable to adaptation; (iii) the dual-weighted residual method, which provides global and element-wise error estimates for quantities of interest; and (iv) a projection-based anisotropic error indicator along with the associated adaptation mechanics that can detect and refine strongly directional features in the physical and/or parameter spaces simultaneously in an efficient manner. Both the spatial and stochastic discretization errors are controlled through the adaptive refinement of the spatial mesh or polynomial chaos expansion degree based on these anisotropic error indicators. We analyze stability, approximation properties, and *a priori* error bounds of the spatio-stochastic adaptive method. We finally demonstrate the effectiveness of our formulation for engineering-relevant transonic turbulent aerodynamics problems with uncertainties in flow conditions and turbulence parameters.

*Keywords:* uncertainty quantification, discontinuous Galerkin methods, sparse polynomial chaos, error estimation, anisotropic adaptivity, aerodynamics

---

## 1. Introduction

A complete characterization of complex engineering systems by numerical simulation requires both the accurate prediction of output quantities of interest as well as the quantification of the associated uncertainties in these predictions. Broadly, two distinct sources of error emerge when making numerical predictions [41]. The first is the discretization error, which lies at the interface of the mathematical model (i.e., the partial differential equations (PDEs)) and the computer model; it is a consequence of the finite-dimensional approximation of the PDEs. The quantification and efficient control of the discretization error using limited computational resources is the goal of error estimation and adaptation [2, 12, 24]. The second is the modeling error, which lies at

---

\*Corresponding author

*Email addresses:* `geoff.donoghue@mail.utoronto.ca` (Geoff Donoghue), `myano@utias.utoronto.ca` (Masayuki Yano)

the interface of physical truth and the mathematical model (i.e., the PDEs); it is a consequence of various uncertainties that may include the operating conditions, geometry, model parameters, and simplifying assumptions made to the governing equations. The quantification of the model error is the goal of the field of uncertainty quantification (UQ) [38, 40, 1, 19, 37], which can be further classified into parametric and non-parametric approaches [60]. The former is restricted to uncertainties inherit in empirical coefficients, operating conditions, or other input parameters; the latter treats more general forms of uncertainties such that those arising from the use of simplified models and equations. This work will focus on the former class of UQ. A prominent approach to parametric UQ is to model the inputs using probability distributions and solve the associated stochastically parameterized partial differential equations (SPDEs). To provide reliable simulation of complex engineering systems in the presence of parametric uncertainties, we must quantify and control the numerical discretization error in both the spatial and parametric approximation spaces. The development and analysis of such a method is the goal of this work. For a discussion of error estimation and adaptive/hierarchical modeling for non-parametric uncertainty quantification, we refer to [44, 54, 43, 14].

From a mathematical point of view, the method we develop and analyze herein can be summarized as an output error estimation and goal-oriented adaptation technique for SPDEs. We here focus on SPDEs that (i) exhibit a wide range of spatial scales, (ii) exhibit strong and general nonlinearity, (iii) are hyperbolic or advection-dominated, and (iv) have a low to moderate number of stochastic parameters. We focus on SPDEs that exhibit these properties because our application interest is in aerodynamics, where the engineering need for a reliable UQ is well recognized but further algorithm development is required to address UQ challenges in practical engineering settings [51, 60, 10, 50]. Within the broad context of uncertainty quantification this work presents a forward method for the rapid quantification of parametric uncertainty. In addition, the focus on low-dimensional parameter spaces precludes the application of this algorithm to non-parametric uncertainties which are perforce infinite-dimensional [60, 20].

Even in the deterministic setting, the reliable and efficient solution of complex PDEs that exhibit features (i)–(iii) is challenging due to the long-range and nonlinear interaction of various features, which in turn engenders high computational cost. SPDEs that exhibit features (i)–(iv) demand the resolution of these features in the presence of uncertainties. One way to overcome this challenge, which has been shown to be effective for deterministic PDEs, is goal-oriented error estimation and adaptation based on the dual-weighted residual (DWR) method [12, 42, 48]; in fact adaptivity is arguably a necessity for the accurate simulation of complex aerodynamics problems [24, 51, 63]. We refer to [2, 24] for reviews of adaptive methods for (deterministic) PDEs and here focus on the review of error estimation and adaptation techniques for SPDEs.

Some existing adaptive methods for SPDEs perform adaptation in the stochastic space only. An early approach—introduced by Wan and Karniadakis—is multi-element generalized PC [56, 57], which tessellates the parameter space and uses polynomial chaos (PC) expansions [59, 28] in each subdomain. This approach is also known as the  $h$ -version of stochastic Galerkin method [7]. *A posteriori* error estimation and adaptation strategies are developed in, e.g., [55, 16]. These works focus on the estimation and control of the discretization error in the stochastic space only; they do not provide a complete picture of the total numerical error in both stochastic *and* physical spaces. While the physical space error may be assumed to be small for simple PDEs, such an assumption rarely holds for complex PDEs that exhibit features (i)–(iii) as discussed above [24].

The idea of spatio-stochastic error estimation and adaptivity, which aims to estimate and control

the errors due to discretization in both the physical and stochastic spaces, has emerged more recently. Almeida and Oden [4] propose goal-oriented adaptive methods that provide both finite element mesh refinement and anisotropic refinement of a stochastic collocation grid. In a series of papers, Eigel et al. consider adaptive solutions of linear elliptic problems using a residual-based error estimator [21, 22] and with a tensor-product decomposition to construct a low-rank approximation of high(er)-dimensional problems [23]. Guignard et al. [32] derive *a posteriori* error estimates for perturbation methods for SPDEs that can be used to drive adaptivity. Guignard and Nobile [31] also consider a residual-based spatio-stochastic adaptive method for stochastic collocation methods [6, 61]. Bespalov et al. [13] similarly consider spatio-stochastic adaptivity for linear elliptic problems, but with goal-oriented adaptation based on the DWR method [12]. Mathelin and Le Maître [39] also consider the DWR-based error estimation and adaptivity with applications in one-dimensional Burgers’ equation. These works are however limited to linear elliptic problems or simple one-dimensional nonlinear PDEs.

More recently, spatio-stochastic error estimation and adaptivity has been applied to more complex problems in fluid dynamics. Bryant et al. [15] consider adaptive solutions of the stochastic incompressible Navier-Stokes equations based on the DWR error estimate,  $h$ -adaptivity in the physical space, and  $p$ -adaptivity in the stochastic space. Barth [10] considers the adaptive solution of aerodynamic flows governed by the compressible Navier-Stokes equations using the DWR error estimate and  $h$ -adaptivity in the physical space, as well as non-intrusive adaptive sparse quadrature in the stochastic space. Van Langenhove et al. [53] also consider goal-oriented spatio-stochastic error control for aerodynamic flows using the DWR error estimate and a continuous metric-based mesh framework in the physical space and a simplex stochastic collocation method in the stochastic space.

The above works [15, 10, 53], like our current work, are motivated by the need to estimate and control the errors due to the physical and stochastic discretizations for practical engineering problems. However, unlike our work, they separate the discretization of the physical and stochastic spaces, and hence do not exploit the spatially dependent stochastic structure of the problem. To the best of the authors’ knowledge, there has not been published work that explores anisotropic combined error control for nonlinear SPDEs with aforementioned features (i)–(iv). The development and analysis of such a method is the overarching goal of this work.

Our spatio-stochastic adaptive solver is based on the discontinuous Galerkin (DG) method [18, 9, 5], which provides stability for advection-dominated PDEs and  $hp$ -flexibility for adaptation. We extend the DG method to include element-wise PC expansions; the DG method permits a rapidly changing PC expansion degree between elements and enables the sparse representation of non-constant PC expansion fields. Given a DG solution to the SPDE, both the spatial and stochastic errors are estimated using the DWR method [12, 42, 48] like many of the aforementioned works [13, 39, 15, 10, 53]. Using the error indicators from the DWR method, the elements with the highest combined spatio-stochastic error are marked for refinement. To determine *how* to best refine these elements from a number of anisotropic spatio-stochastic refinement options, we employ a local solver, inspired by those used in anisotropic adaptive DG methods [25, 34, 17, 62]; given several anisotropic refinement options, we deduce the most efficient refinement option based on error reduction per degree of freedom incurred. The resulting algorithm fully exploits the localized anisotropic spatio-stochastic structure in the SPDE. As we will later demonstrate, this automatic computation of sparse PC expansion fields enables both rapid convergence in the output quantity of interest and significant runtime speedup.

We summarize the threefold contributions of this work. The first contribution is the development of the aforementioned goal-oriented anisotropic spatio-stochastic adaptive DG method for SPDEs. The formulation employs an element-wise discontinuous PC expansion and a local solver to exploit spatio-stochastic anisotropy and sparsity. The second contribution is the analysis of the stability and quasi-optimality of the stochastic DG method and the approximation properties of the associated spatio-stochastic polynomial spaces. The analysis shows the need for combined error estimation as well as anisotropic spatio-stochastic adaptivity to efficiently solve SPDEs and inform the design of the adaptation strategy. The third contribution is the demonstration of the method for a two-dimensional advection-diffusion equation and transonic Reynolds-averaged Navier-Stokes flows past an airfoil. Through the judicious construction and refinement of our spatio-stochastic approximation spaces, the method achieves significant computational complexity reduction compared to non-adaptive stochastic Galerkin methods. The threefold contributions provide steps towards reliable uncertainty quantification of complex engineering problems.

Before we conclude the introduction, we note a limitation of the present work. Our adaptive stochastic DG method is designed for problems that exhibit a wide range of spatial scales and nonlinearity but only a few stochastic parameters. The method in particular suffers from the curse of dimensionality. The method is unsuitable for high- or infinite-dimensional problems that often arise from SPDEs with random fields. In such problems, the Monte-Carlo method, and its variants such as multi-level Monte-Carlo [30], remains a more effective choice.

The remainder of this paper is organized as follows. In Section 2, we introduce a DG method for SPDEs that supports spatially varying, element-wise PC expansions. In Section 3, we provide a spatio-stochastic *a priori* error analysis of the DG method for stochastic advection-diffusion-reaction equations; the analysis extends the anisotropic *hp* error analysis for deterministic DG methods by Georgoulis, Hall, Hartmann, and Houston in a series of papers [36, 25, 26, 27, 34] to SPDEs. In Section 4, we introduce an anisotropic spatio-stochastic adaptive DG method informed by the DWR error estimate and local solves. Section 5 demonstrates spatio-stochastic adaptation for the advection-diffusion equation and transonic aerodynamic flows.

## 2. Stochastic discontinuous Galerkin method

In this section, we present a DG method for SPDEs that supports spatially varying, element-wise PC expansions. Specifically, we introduce the spatio-stochastic approximation space, the associated DG method, and its efficient implementation.

### 2.1. Problem statement

We present an abstract form of the stochastically parametrized PDEs associated with systems of nonlinear conservation laws. We first introduce a  $d$ -dimensional physical domain  $\Omega \subset \mathbb{R}^d$  with a Lipschitz boundary. We next introduce a probability space  $(\Xi, \mathcal{B}(\Xi), \mathbb{P}_\xi)$ , where  $\Xi \subset \mathbb{R}^P$  is the  $P$ -dimensional sample space,  $\mathcal{B}(\Xi)$  is the Borel  $\sigma$ -algebra generated by  $\Xi$ , and  $\mathbb{P}_\xi$  is the probability measure. Throughout this work, our sample space  $\Xi$  is taken to be a product space (implying the assumption of statistically independent input parameters) and hence can be expressed as  $\Xi = \prod_{n=1}^P \Xi_n$  for  $\Xi_n \subset \mathbb{R}$ ,  $n = 1, \dots, P$ . We then seek an  $m$ -component real-valued random field  $u : \Omega \times \Xi \rightarrow \mathbb{R}^m$  that satisfies a system of  $m$  SPDEs,

$$\nabla \cdot (\mathcal{F}^c(u, x; \xi) - \mathcal{F}^v(u, \nabla u, x; \xi)) = \mathcal{S}(u, \nabla u, x; \xi) \quad \text{a.e. in } \Omega \times \Xi,$$

along with appropriate boundary conditions; here  $\mathcal{F}^c : \mathbb{R}^m \times \Omega \times \Xi \rightarrow \mathbb{R}^m$  is the convective flux,  $\mathcal{F}^v : \mathbb{R}^m \times \mathbb{R}^{m \times d} \times \Omega \times \Xi \rightarrow \mathbb{R}^{m \times d}$  is the viscous flux, and  $\mathcal{S} : \mathbb{R}^m \times \mathbb{R}^{m \times d} \times \Omega \times \Xi \rightarrow \mathbb{R}^m$  is the source term. Given the solution  $u : \Omega \times \Xi \rightarrow \mathbb{R}^m$  to the SPDE, we wish to evaluate statistics associated with some quantity of interest:

$$\mathcal{J}(u) \equiv \int_{\Xi} g(\mathcal{J}(u(\cdot; \xi); \xi)) d\mathbb{P}_{\xi}, \quad (1)$$

where  $\mathcal{J}(u(\cdot; \xi); \xi)$  is the quantity of interest evaluated for the particular value of the parameter  $\xi \in \Xi$ , and  $g : \mathbb{R} \times \Xi \rightarrow \mathbb{R}$  is the transformation required to evaluate the particular statistics; e.g.,  $g(\mathcal{J}(u(\cdot; \xi))) \equiv \mathcal{J}(u(\cdot; \xi))$  for the mean. The goal of work is to approximate  $\mathcal{J}(u)$  as efficiently as possible (i.e., for a minimal computational cost at a given accuracy) and to equip the approximation with an *a posteriori* error estimate.

## 2.2. Element-wise adaptive spatio-stochastic polynomial space

We now describe the spatio-stochastic polynomial space used in our DG method for SPDEs. To this end, we first introduce a triangulation  $\mathcal{T}_h$  that comprises the set  $\{\kappa_i\}$  of non-overlapping polygonal elements that tessellate the physical domain  $\Omega$ ; the triangulation may contain hanging nodes. We next introduce a set of element-wise physical polynomial degrees  $\{p^\kappa \in \mathbb{Z}_{\geq 0}\}_{\kappa \in \mathcal{T}_h}$ . Using this notation, the (physical) *hp* space suitable for DG approximation can be written as

$$\mathcal{V}_{h,p} \equiv \{v \in L^2(\Omega)^m \mid v|_{\kappa} \in \mathcal{P}^{p^\kappa}(\kappa)^m, \forall \kappa \in \mathcal{T}_h\}, \quad (2)$$

where  $L^2(\Omega)$  denotes the standard Lebesgue space of square integrable functions, and  $\mathcal{P}^{p^\kappa}(\kappa)$  denotes the space of degree  $p^\kappa$  polynomials over element  $\kappa \subset \Omega$ . Similarly, we introduce a set of multi-indices  $\{s^\kappa \in \mathbb{Z}_{\geq 0}^P\}_{\kappa \in \mathcal{T}_h}$  that describe the element-wise stochastic polynomial degrees. Note that we describe the stochastic polynomial space on each element  $\kappa$  using the *P*-component multi-index  $s^\kappa \equiv (s_1^\kappa, \dots, s_P^\kappa)$  as we consider PC expansions of differing degrees in each of the *P* stochastic dimensions. The spatio-stochastic space in which we seek the solution is given by

$$\mathcal{V}_{h,p,s} \equiv \{v \in L^2(\Omega \times \Xi)^m \mid v|_{\kappa} \in (\mathcal{P}^{p^\kappa}(\kappa) \otimes \mathcal{P}^{s^\kappa}(\Xi))^m, \forall \kappa \in \mathcal{T}_h\}, \quad (3)$$

where, following the standard multi-index convention,

$$\mathcal{P}^{s^\kappa \equiv (s_1^\kappa, \dots, s_P^\kappa)}(\Xi) = \mathcal{P}^{s_1^\kappa}(\Xi_1) \otimes \dots \otimes \mathcal{P}^{s_P^\kappa}(\Xi_P)$$

is the space of tensor-product multi-variate polynomials on the product space  $\Xi \equiv \prod_{n=1}^P \Xi_n$ . The space  $\mathcal{V}_{h,p,s}$  can be more compactly expressed as  $\mathcal{V}_{h,p,s} = \bigoplus_{\kappa \in \mathcal{T}_h} (\mathcal{P}^{p^\kappa}(\kappa) \otimes \mathcal{P}^{s^\kappa}(\Xi))^m$ . We emphasize that, for a given element  $\kappa \in \mathcal{T}_h$ , the variation in the solution in the physical space  $\kappa \subset \Omega \subset \mathbb{R}^d$  is sought in  $\mathcal{P}^{p^\kappa}(\kappa)$  and the variation in the solution in the stochastic space  $\Xi \subset \mathbb{R}^P$  is sought in  $\mathcal{P}^{s^\kappa}(\Xi)$ . Because we consider a discontinuous approximation space as in the DG method, we can readily support elementally varying physical polynomial degrees  $p^\kappa$  and stochastic polynomial degree  $s^\kappa$ ; we will leverage this property to support adaptive *s*-refinement (but we will not exploit adaptive *p*-refinement in this work).

For clarity, we now present more explicit representations of functions in  $\mathcal{V}_{h,p,s}$  in terms of its basis. To this end, we first introduce a basis  $\{\phi_i^\kappa : \kappa \rightarrow \mathbb{R}\}_{i=1}^{N_{p^\kappa}}$  for the physical polynomial space  $\mathcal{P}^{p^\kappa}(\kappa)$  of dimension  $N_{p^\kappa}$ . We next introduce a basis  $\{\psi_j : \Xi_n \rightarrow \mathbb{R}\}_{j=0}^{s_n^\kappa}$  for the *n*-th stochastic

dimension for all  $n = 1, \dots, P$ . Because of its tensor-product structure, the basis for  $\mathcal{P}^{s^\kappa}(\Xi)$  can be constructed from the product  $\psi_{j \equiv (j_1, \dots, j_P)}(\xi \equiv (\xi_1, \dots, \xi_P)) = \psi_{j_1}(\xi_1) \cdots \psi_{j_P}(\xi_P)$  for  $j \leq s^\kappa$ , where  $j \leq s^\kappa$  denotes multi-index  $j$  that satisfies  $j_n \leq s_n^\kappa$ , for all  $n = 1, \dots, P$ . We denote the stochastic basis for element  $\kappa \in \mathcal{T}_h$  by  $\{\psi_j : \Xi \rightarrow \mathbb{R}\}_{j \leq s^\kappa}$  and its cardinality by  $N_{s^\kappa} \equiv \prod_{n=1}^P (s_n^\kappa + 1)$ . Any function  $v_{h,p,s} \in \mathcal{V}_{h,p,s}$  restricted to element  $\kappa \in \mathcal{T}_h$  belongs to the space  $(\mathcal{P}^{s^\kappa}(\kappa) \otimes \mathcal{P}^{s^\kappa}(\Xi))^m$ ; the  $k$ -th component of such a function evaluated at  $(x, \xi) \in \kappa \times \Xi$  can be expressed using the basis as

$$v_{h,p,s}|_\kappa(x, \xi)_k = \sum_{j \leq s^\kappa} \sum_{i=1}^{N_{p^\kappa}} \hat{v}_{i,j,k}^\kappa \phi_i^\kappa(x) \psi_j(\xi) = \sum_{j_1=1}^{s_1^\kappa} \cdots \sum_{j_P=1}^{s_P^\kappa} \sum_{i=1}^{N_{p^\kappa}} \hat{v}_{i,(j_1, \dots, j_P),k}^\kappa \phi_i^\kappa(x) \psi_{i_1}(\xi_1) \cdots \psi_{i_P}(\xi_P)$$

for coefficients  $\{\{\{\hat{v}_{i,j,k}^\kappa\}_{i=1}^{N_{p^\kappa}}\}_{j \leq s^\kappa}\}_{k=1}^m$  of cardinality  $mN_{s^\kappa}N_{p^\kappa}$ .

Combining the expressions for all elements in  $\mathcal{T}_h$ , the  $k$ -th component of the function evaluated at  $(x, \xi) \in \Omega \times \Xi$  can be expressed as

$$v_{h,p,s}(x, \xi)_k = \bigoplus_{\kappa \in \mathcal{T}_h} \sum_{j \leq s^\kappa} \sum_{i=1}^{N_{p^\kappa}} \hat{v}_{i,j,k}^\kappa \phi_i^\kappa(x) \psi_j(\xi),$$

for coefficients  $\{\{\{\{\hat{v}_{i,j,k}^\kappa\}_{i=1}^{N_{p^\kappa}}\}_{j \leq s^\kappa}\}_{k=1}^m\}_{\kappa \in \mathcal{T}_h}$  of cardinality  $N_{\mathcal{N}} \equiv \sum_{\kappa \in \mathcal{T}_h} mN_{s^\kappa}N_{p^\kappa}$ . Again, due to the use of the discontinuous approximation space, the coefficients for each element can be varied independently of one another without any inter-elemental constraints.

**Remark 1.** A spatio-stochastic function  $v_{h,p,s} \in \mathcal{V}_{h,p,s}$  with spatially varying stochastic polynomial degrees can also be interpreted as (global) PC expansion with sparse “mode strengths.” To this end, let the  $P$ -tuple  $s^{\max}$  be a multi-index such that  $s_n^{\max} \geq \max_{\kappa \in \mathcal{T}_h} s_n^\kappa$ ,  $n = 1, \dots, P$ ; i.e.,  $s_n^{\max}$  is the maximum polynomial degree for the  $n$ -th stochastic dimension used anywhere in the domain. Then, we may express  $v_{h,p,s} \in \mathcal{V}_{h,p,s}$  as

$$v_{h,p,s} = \sum_{j \leq s^{\max}} v_{h,p}^{(j)}(x) \psi_j(\xi) \equiv \sum_{j \leq s^{\max}} \left[ \bigoplus_{\kappa \in \mathcal{T}_h} (E^\kappa \hat{v}^\kappa)_{i,j}^\kappa \phi_i^\kappa(x) \right] \psi_j(\xi),$$

where  $v_{h,p}^{(j)} \in \mathcal{V}_{h,p}$  is the mode strength given by the expression in the brackets, and  $E^\kappa : \mathbb{R}^{mN_{s^\kappa}N_{p^\kappa}} \rightarrow \mathbb{R}^{mN_{s^{\max}}N_{p^\kappa}}$  is the prolongation operator such that  $(E^\kappa \hat{v})_{i,j} = \hat{v}_{i,j}$  for  $j \leq s^\kappa$  and  $(E^\kappa \hat{v})_{i,j} = 0$  otherwise. In other words,  $E^\kappa$  simply “pads” the coefficients  $\hat{v}^\kappa$  with 0 such that the dimension is compatible with the maximum degree of the stochastic polynomial used over the domain  $s^{\max}$ . The resulting mode strengths are sparse in the sense that the mode strength for the multi-index  $j$  vanishes for elements whose stochastic polynomial degree  $s^\kappa$  yields  $j \not\leq s^\kappa$ .

### 2.3. Stochastic discontinuous Galerkin method

Having defined the approximation space  $\mathcal{V}_{h,p,s}$ , we now introduce the projection method that we use to find the solution  $u_{h,p,s} \in \mathcal{V}_{h,p,s}$ . To this end, we first recall that the (non-stochastic) DG approximation for a parametrized PDE evaluated at a fixed parameter  $\xi \in \Xi$  can be compactly expressed as follows: find  $u_{h,p} \in \mathcal{V}_{h,p}$  such that

$$\mathcal{R}_{h,p}(u_{h,p}, v_{h,p}; \xi) = 0 \quad \forall v_{h,p} \in \mathcal{V}_{h,p},$$

where  $\mathcal{R}_{h,p}(\cdot, \cdot; \xi) : \mathcal{V}_{h,p} \times \mathcal{V}_{h,p} \rightarrow \mathbb{R}$  is the semi-linear form associated with the particular DG approximation, and  $\mathcal{V}_{h,p}$  is the (non-stochastic) DG space (2). Given  $u_{h,p} \in \mathcal{V}_{h,p}$  for the specific value of the parameter  $\xi \in \Xi$ , the associated quantity of interest is given by  $\mathcal{J}_{h,p}(u_{h,p}; \xi)$ , where  $\mathcal{J}_{h,p}(\cdot, \xi) : \mathcal{V}_{h,p} \rightarrow \mathbb{R}$  is the DG approximation of the output functional. For brevity, we omit a complete presentation of the DG formulation and refer to review papers [18, 5] and textbooks [35, 47]; we merely note that, in this work, we use a “standard” DG method with an upwind numerical flux for the convection term, the so-called BR2 scheme [11] for the diffusion term, and an asymptotically dual-consistent discretization of the source term [45].

To obtain a spatio-stochastic DG approximation, we perform Galerkin projection in the stochastic space to obtain the following: find  $u_{h,p,s} \in \mathcal{V}_{h,p,s}$  such that

$$\mathcal{R}_{h,p,s}(u_{h,p,s}, v_{h,p,s}) = 0 \quad \forall v_{h,p,s} \in \mathcal{V}_{h,p,s}, \quad (4)$$

where the spatio-stochastic DG residual form is expressed as

$$\mathcal{R}_{h,p,s}(w_{h,p,s}, v_{h,p,s}) \equiv \int_{\Xi} \mathcal{R}_{h,p}(w_{h,p,s}(\cdot, \xi), v_{h,p,s}(\cdot, \xi); \xi) d\mathbb{P}_{\xi} \quad \forall w_{h,p,s}, v_{h,p,s} \in \mathcal{V}_{h,p,s}.$$

Given  $u_{h,p,s} \in \mathcal{V}_{h,p,s}$ , the associated quantity of interest is taken to be

$$J_{h,p,s} \equiv \mathcal{J}(u_{h,p,s}),$$

where the spatio-stochastic output functional is given by

$$\mathcal{J}_{h,p,s}(w_{h,p,s}) \equiv \int_{\Xi} g(\mathcal{J}_{h,p}(w_{h,p,s}(\cdot, \xi); \xi)) d\mathbb{P}_{\xi} \quad \forall w_{h,p,s} \in \mathcal{V}_{h,p,s},$$

with  $g : \mathbb{R} \times \Xi \rightarrow \mathbb{R}$  being the transformation associated with the particular statistics, as introduced in (1).

#### 2.4. Computational implementation

We now present an implementation of the stochastic DG method that builds on an existing DG method for non-stochastic problems. To begin, we first recall that any function  $v_{h,p,s} \in \mathcal{V}_{h,p,s}$  is identified with unique coefficients  $\{\{\{\{\hat{v}_{i,j,k}^{\kappa}\}_{i=1}^{N_{p^{\kappa}}}\}_{j \leq s^{\kappa}}\}_{k=1}^m\}_{\kappa \in \mathcal{T}_h}$  of cardinality  $N_{\mathcal{N}} \equiv \sum_{\kappa \in \mathcal{T}_h} m N_{s^{\kappa}} N_{p^{\kappa}}$  by

$$v_{h,p,s}(x, \xi)_k = \bigoplus_{\kappa \in \mathcal{T}_h} \sum_{j \leq s^{\kappa}} \sum_{i=1}^{N_{p^{\kappa}}} \hat{v}_{i,j,k}^{\kappa} \phi_i^{\kappa}(x) \psi_j(\xi).$$

The coefficients are identified by four indices: the element index  $\kappa \in \mathcal{T}_h$ ; the equation component index  $k \in [1, m]$ ; the stochastic basis index  $j \leq s^{\kappa}$ , which is a  $P$ -tuple; and the spatial basis index  $i \in [1, N_{p^{\kappa}}]$ . In practice, we store the fourth-order tensor of coefficient as a flattened vector  $\mathbf{V}_{h,p,s} \in \mathbb{R}^{N_{\mathcal{N}}}$ , with  $\kappa$  as the outermost (i.e., slowest changing) index, followed by  $k$ , then  $j$ , and  $i$  as the innermost (i.e., fastest changing) index; i.e.,  $(\mathbf{V}_{h,p,s})_{(\kappa,k,j,i)} = \{\{\{\{\hat{v}_{i,j,k}^{\kappa}\}_{i=1}^{N_{p^{\kappa}}}\}_{j \leq s^{\kappa}}\}_{k=1}^m\}_{\kappa \in \mathcal{T}_h}$ . For instance, suppose we discretize a two-component ( $m = 2$ ) equation in one-dimensional physical space ( $d = 1$ ) and one-dimensional stochastic space ( $P = 1$ ) using the physical and stochastic

polynomial degree of  $p^{\kappa_0} = 2$  and  $s^{\kappa_0} = (1)$  for the first element and  $p^{\kappa_1} = 1$  and  $s^{\kappa_1} = (2)$  for the second element. The associated flattened vector in  $\mathbf{V}_{h,p,s} \in \mathbb{R}^{N_{\mathcal{N}}=24}$  is organized as

$$\mathbf{V}_{h,p,s} = \left[ \begin{array}{c} \begin{array}{cc} & \kappa_0 \\ & c_0 \quad c_1 \\ \psi_0 & \psi_1 \\ [\phi_0\phi_1\phi_2] & [\phi_0\phi_1\phi_2] \end{array} \\ \begin{array}{cc} & \kappa_1 \\ & c_0 \quad c_1 \\ \psi_0 & \psi_1 & \psi_2 \\ [\phi_0\phi_1] & [\phi_0\phi_1] & [\phi_0\phi_1] \end{array} \end{array} \right].$$

The particular ordering provides two computational advantages: the Jacobian matrix has a element-wise block structure, which facilitates both preconditioning and straightforward parallel implementation and the ordering allows for the potential to use different physical and/or stochastic polynomial degrees for each component of the equation, though we do not exploit this flexibility in this work.

We next consider the solution of the spatio-stochastic DG problem (4). The problem written in terms of the aforementioned basis coefficients is as follows: find the coefficients  $\{\{\{\{\hat{u}_{i,j,k}^{\kappa}\}_{i=1}^{N_{p^{\kappa}}}\}_{j \leq s^{\kappa}}\}_{k=1}^m\}_{\kappa \in \mathcal{T}_h}$  such that  $u_{h,p,s} = \bigoplus_{\kappa \in \mathcal{T}_h} \sum_{j \leq s^{\kappa}} \sum_{i=1}^{N_{p^{\kappa}}} \hat{u}_{i,j}^{\kappa} \phi_i^{\kappa} \psi_j$  satisfies

$$\mathcal{R}_{h,p,s}(u_{h,p,s}, e_k \phi_i^{\kappa} \otimes \psi_j) = 0$$

for all  $i \in \{1, \dots, N_{p^{\kappa}}\}$ ,  $j \leq s^{\kappa}$ ,  $k \in \{1, \dots, m\}$ , and  $\kappa \in \mathcal{T}_h$ , where  $e_k \in \mathbb{R}^m$  is the  $k$ -th standard unit vector. In practice, we approximate the integral in  $\mathcal{R}_{h,p,s}(\cdot, \cdot)$  over the sample space  $\Xi \subset \mathbb{R}^P$  with an elementally varying  $Q^{\kappa}$ -point quadrature rule so that

$$\mathcal{R}_{h,p,s}(u_{h,p,s}, e_k \phi_i^{\kappa} \otimes \psi_j) \approx \sum_{q=1}^{Q^{\kappa}} \omega_q [\mathcal{R}_{h,p}(u_{h,p,s}(\cdot, \xi_q), e_k \otimes \phi_i^{\kappa}; \xi_q)] \psi_j(\xi_q), \quad (5)$$

where the elemental stochastic quadrature order is chosen based on the stochastic polynomial degree of the element and its neighbors to enable efficient residual evaluation. Furthermore, in the view of Remark 1, the solution evaluated at a quadrature point  $\xi_q \in \Xi$ ,  $u_{h,p,s}(\cdot, \xi_q) \in \mathcal{V}_{h,p}$ , results from a linear combination of the ‘‘sparse’’ mode strengths

$$u_{h,p,s}(x, \xi_q) = \sum_{j \leq s^{\max}} u_{h,p}^{(j)}(x) \psi_j(\xi_q). \quad (6)$$

Hence, given a spatio-stochastic function  $u_{h,p,s} \in \mathcal{V}_{h,p,s}$ , the evaluation of the spatio-stochastic residual  $\mathcal{R}_{h,p,s}(u_{h,p,s}, e_k \phi_i^{\kappa} \otimes \psi_j)$  proceeds in three steps: (i) we first evaluate the (non-stochastic) function  $u_{h,p,s}(\cdot, \xi_q) \in \mathcal{V}_{h,p}$  associated with the stochastic quadrature point  $\xi_q \in \Xi$  using (6); (ii) we next evaluate the standard, deterministic DG residual  $\mathcal{R}_{h,p}(u_{h,p,s}(\cdot, \xi_q), e_k \otimes \phi_i^{\kappa}; \xi_q)$  as shown in the bracket of (5); (iii) we repeat (i) and (ii) for all  $Q^{\kappa}$  stochastic quadrature points to evaluate (5).

Using the aforementioned flattened vector, the residual operator can also be expressed as  $\mathbf{R}_{h,p,s} : \mathbb{R}^{N_{\mathcal{N}}} \rightarrow \mathbb{R}^{N_{\mathcal{N}}}$  whose entries are given by

$$\mathbf{R}_{h,p,s}(\mathbf{U}_{h,p,s})_{(\kappa,k,i,j)} \equiv \mathcal{R}_{h,p,s}(u_{h,p,s}, e_k \phi_i^{\kappa} \otimes \psi_j).$$

Equivalently,

$$\mathbf{R}_{h,p,s}(\mathbf{U}_{h,p,s})_{(\kappa,k,i,j)} = \sum_{q=1}^{Q^{\kappa}} \omega_q \mathbf{R}_{h,p}(\mathbf{U}_{h,p}(\xi_q); \xi_q)_{(\kappa,k,i)} \psi_j(\xi_q)$$

for  $\mathbf{U}_{h,p}(\xi_q) = \sum_{j \leq s^{\max}} \mathbf{U}_{h,p}^{(j)} \psi_j(\xi_q)$ , where  $\mathbf{U}_{h,p}^{(j)}$  is the vector of coefficients associated with  $u_{h,p}^{(j)}$ —that is, the deterministic solution evaluated at the  $q^{\text{th}}$  quadrature point, and  $\mathbf{R}_{h,p}(\mathbf{U}_{h,p}(\xi_q); \xi_q)_{(\kappa,k,i)} \equiv \mathcal{R}_{h,p}(u_{h,p}^{(j)}, e_k \phi_i^k; \xi_q)$  is the deterministic algebraic DG residual evaluated at  $\xi_q$ . In this algebraic form, the DG problem (4) is equivalent to finding  $\mathbf{U}_{h,p,s} \in \mathbb{R}^{N_{\mathcal{N}}}$  such that  $\mathbf{R}_{h,p,s}(\mathbf{U}_{h,p,s}) = 0$  in  $\mathbb{R}^{N_{\mathcal{N}}}$ .

We make two observations about the spatio-stochastic residual evaluation procedure. We first observe that the number of deterministic DG residual evaluations for a given element  $\kappa$  is equal to the number of stochastic quadrature points  $Q^\kappa$  used to approximate the stochastic integral. Secondly, we observe that the scheme is “semi-intrusive” in the sense that it requires the access to the element-wise deterministic DG residual for an efficient implementation that exploits spatially varying physical and stochastic approximation polynomial degrees.

We will solve the nonlinear algebraic system (4) using a Newton(-like) method which requires the Jacobian of the residual. Similarly to the residual, the spatio-stochastic Jacobian can be constructed from the associated (non-stochastic) Jacobian: i.e.,

$$\mathcal{R}'_{h,p,s}(u_{h,p,s}; e_{k'} \phi_{i'}^{k'} \otimes \psi_{j'}, e_k \phi_i^k \otimes \psi_j) = \sum_{q=1}^{Q^\kappa} \omega_q \left[ \mathcal{R}'_{h,p}(u_{h,p,s}(\cdot, \xi_q); e_{k'} \phi_{i'}^{k'}, e_k \phi_i^k; \xi_q) \right] \psi_{j'}(\xi_q) \psi_j(\xi_q), \quad (7)$$

for  $i, i' \in \{1, \dots, N_{p^\kappa}\}$ ,  $j, j' \leq s^\kappa$ ,  $k, k' \in \{1, \dots, m\}$ , and  $\kappa, \kappa' \in \mathcal{T}_h$ . The evaluation of the spatio-stochastic Jacobian again proceeds in three steps: (i) we first evaluate the (non-stochastic) function  $u_{h,p,s}(\cdot, \xi_q) \in \mathcal{V}_{h,p}$  associated with the stochastic quadrature point  $\xi_q \in \Xi$  using (6); (ii) we next evaluate the standard, deterministic DG Jacobian  $\mathcal{R}'_{h,p}(u_{h,p,s}(\cdot, \xi_q); e_{k'} \phi_{i'}^{k'}, e_k \phi_i^k; \xi_q)$  as shown in the bracket of (7); (iii) we repeat (i) and (ii) for all  $Q^\kappa$  stochastic quadrature points to evaluate (7). The Jacobian is element-wise block sparse, where each block is of the size  $m N_{p^\kappa} N_{s^\kappa}$ . We further note that since the DG residual depends on the inter-elemental jump between neighboring elements, the Jacobian will also be nonzero when  $\kappa$  and  $\kappa'$  share an elemental boundary.

Using the aforementioned flattened vector, the Jacobian operator can also be expressed as  $\partial \mathbf{R}_{h,p,s} : \mathbb{R}^{N_{\mathcal{N}}} \rightarrow \mathbb{R}^{N_{\mathcal{N}} \times N_{\mathcal{N}}}$  whose entries are given by

$$\partial \mathbf{R}_{h,p,s}(\mathbf{U}_{h,p,s})_{(\kappa,k,i,j),(\kappa',k',i',j')} = \mathcal{R}'_{h,p,s}(u_{h,p,s}; e_{k'} \phi_{i'}^{k'} \otimes \psi_{j'}, e_k \phi_i^k \otimes \psi_j),$$

or, equivalently,

$$\partial \mathbf{R}_{h,p,s}(\mathbf{U}_{h,p,s})_{(\kappa,k,i,j),(\kappa',k',i',j')} = \sum_{q=1}^{Q^\kappa} \omega_q \partial \mathbf{R}_{h,p}(\mathbf{U}_{h,p}(\xi_q))_{(\kappa,k,i),(\kappa',k',i')} \psi_j(\xi_q) \psi_{j'}(\xi_q),$$

where  $\partial \mathbf{R}_{h,p}(\mathbf{U}_{h,p}(\xi_q); \xi_q)_{(\kappa,k,i),(\kappa',k',i')} = \mathcal{R}'_{h,p}(u_{h,p}^{(j)}; e_{k'} \phi_{i'}^{k'}, e_k \phi_i^k; \xi_q)$  is the deterministic algebraic DG residual evaluated at  $\xi_q$ . The evaluation of the residual and Jacobian is summarized in Algorithm 1.

We solve the nonlinear algebraic system (5) using a pseudo-time continuation (PTC) solver. The (pseudo) time-dependent equation takes on the following form (assuming  $u_h$  is the conservative variable): find  $u_h^{\text{ptc}}(t) \in \mathcal{V}_{h,p,s}$  such that

$$\int_{\Xi} \int_{\Omega} v_{h,p,s} \partial_t u_{h,p,s}^{\text{ptc}} |t dx d\mathbb{P}_\xi + \mathcal{R}_{h,p,s}(u_{h,p,s}^{\text{ptc}}(t), v_{h,p,s}) = 0 \quad \forall v_{h,p,s} \in \mathcal{V}_{h,p,s}, \forall t \in \mathbb{R}_{>0},$$

with  $u_{h,p,s}^{\text{ptc}}(t=0) = u_{h,p,s}^0$  as the initial condition, which is often the freestream condition for aerodynamic flows. The PTC equation is discretized using the backward Euler method. The

---

**Algorithm 1** Stochastic residual and Jacobian evaluation
 

---

**Input:**

 SDG coefficients:  $\mathbf{U}_{h,p,s}$ 
**Output:**

 SDG residual:  $\mathbf{R}_{h,p,s}(\mathbf{U}_{h,p,s})$ 

 SDG Jacobian:  $\partial\mathbf{R}_{h,p,s}(\mathbf{U}_{h,p,s})$ 

- 1: **for**  $\kappa \in \mathcal{T}_h$  **do**
  - 2:   **for**  $\xi_q = 1, 2, \dots, Q^\kappa$  **do**
  - 3:     Evaluate state at  $\xi_q$ :  $\mathbf{U}_{h,p}(\xi_q) = \sum_{j \leq s^{\max}} (\mathbf{U}_{h,p,s})_{(\kappa,i,j,k)} \psi_j(\xi_q)$
  - 4:     Evaluate deterministic residual  $\mathbf{R}_{h,p}(\mathbf{U}_{h,p}(\xi_q); \xi_q)$  and Jacobian  $\partial\mathbf{R}_{h,p}(\mathbf{U}_{h,p}(\xi_q); \xi_q)$
  - 5:     Update residual and Jacobian:
 
$$\begin{aligned} \mathbf{R}_{h,p,s}(\mathbf{U}_{h,p,s})_{(\kappa,k,j,i)} &+= \omega_q \mathbf{R}_{h,p}(\mathbf{U}_{h,p}(\xi_q); \xi_q)_{(\kappa,k,i)} \psi_j(\xi_q) \\ \partial\mathbf{R}_{h,p,s}(\mathbf{U}_{h,p,s})_{(\kappa,k,j,i),(\kappa',k',j',i')} &+= \omega_q \partial\mathbf{R}_{h,p}(\mathbf{U}_{h,p}(\xi_q); \xi_q)_{(\kappa,k,i),(\kappa',k',i')} \psi_j(\xi_q) \psi_{j'}(\xi_q) \end{aligned}$$
- 

linearized equation that arises at each (pseudo) time step is solved using the GMRES method [49] preconditioned with block ILU(0) with minimum-discarded fill reordering [46]. At each (pseudo) time step, we monitor the change in the density and pressure at all spatial and stochastic quadrature points to ensure the physicality of the solution. We refer to [63] for details of the PTC method.

Finally, we note that the output is evaluated as

$$\mathcal{I}_{h,p,s}(u_{h,p,s}) \simeq \sum_{\kappa \in \mathcal{T}_h} \sum_{q=1}^{Q^\kappa} \omega_q g \left( \mathcal{J}_{h,p} \left( \sum_{j \leq s^\kappa} u_{h,p}^{(j)} |_{\kappa} \psi_j(\xi_q); \xi_q \right) \right),$$

which also requires a number of deterministic evaluations equal to the number of stochastic quadrature points.

### 3. Analysis of anisotropic adaptive spatio-stochastic DG method

This section provides *a priori* error analysis of the spatio-stochastic adaptive DG method. We focus solely on the analysis of the advection-diffusion-reaction equation for three reasons. First, the equation exhibits many of the challenges outlined in the introduction, including convection-dominance and widely ranging scales. Second, the equation is linear and is amenable to analysis. Third, the equation has been extensively studied for deterministic DG methods by Georgoulis, Hall, Hartmann, and Houston in a series of papers [36, 25, 26, 27, 34], and much of our analysis for the spatio-stochastic method builds on existing technical tools in these works. We introduce the equation in Section 3.1, provide approximation theory for general anisotropic spatio-stochastic spaces 3.2, and provide *a priori* error estimates for quantities of interest in Section 3.3.

#### 3.1. Model problem: stochastic advection-diffusion-reaction equation

We first introduce a stochastic version of the advection-diffusion-reaction equation considered in [36, 25, 34]. First, for simplicity, we assume that the sample space is unit hypercube  $\Xi \equiv [0, 1]^P$  and the associated probability measure is uniform. We next introduce an advection-diffusion-reaction equation of the following form:

$$-\nabla \cdot (a \nabla u) + \nabla \cdot (bu) + cu = f \quad \text{a.e. in } \Omega \times \Xi,$$

where  $a \in L^\infty(\Xi; L^\infty(\Omega))^{d \times d}$  is a piecewise continuous diffusivity field that is uniformly elliptic in  $\overline{\Omega}$  for each  $\xi \in \Xi$ ,  $b \in L^\infty(\Xi; L^\infty(\Omega))^d$  is a Lipschitz continuous advection field for each  $\xi \in \Xi$ ,  $c \in L^\infty(\Xi; L^\infty(\Omega))$  is a reaction field, and  $f \in L^\infty(\Xi; L^2(\Omega))$  is a source term. We denote the boundary of  $\Omega$  by  $\Gamma$ , and partition  $\Gamma$  into non-overlapping Dirichlet boundary  $\Gamma_D$  and Neumann boundary  $\Gamma_N$  sections. We assume that all Neumann boundaries are outflow in the sense that  $b \cdot n \geq 0$  on  $\Gamma_N$ . The boundary conditions are given by  $u = g_D(\xi)$  on  $\Gamma_D$  and  $n \cdot a \nabla u = g_N(\xi)$  on  $\Gamma_N$ . We assume that the usual positivity hypothesis  $c(\xi) + \frac{1}{2} \nabla \cdot b(\xi) \geq 0$  holds a.e. in  $\Omega$  for each  $\xi \in \Xi$ .

The DG approximation of the advection-diffusion-reaction equation for a fixed parameter  $\xi \in \Xi$  is as follows: find  $u_{h,p} \in \mathcal{V}_{h,p}$  such that

$$\mathcal{B}_{h,p}(u_{h,p}, v_{h,p}; \xi) = \mathcal{L}_{h,p}(v_{h,p}; \xi) \quad \forall v_{h,p} \in \mathcal{V}_{h,p},$$

where the parametrized bilinear form  $\mathcal{B}_{h,p}(\cdot, \cdot; \xi)$  and linear form  $\mathcal{L}_{h,p}(\cdot; \xi)$  are given by [36, 25, 34]

$$\begin{aligned} \mathcal{B}_{h,p}(w, v; \xi) &\equiv \int_{\Omega} (a(\xi) \nabla v \cdot \nabla w - \nabla v \cdot b(\xi) w + c(\xi) w v) dx \\ &\quad + \sum_{\kappa \in \mathcal{T}_h} \left( \int_{\partial_+ \kappa} n \cdot b(\xi) v^+ w^+ ds + \int_{\partial_- \kappa \setminus \Gamma} n \cdot b(\xi) v^+ w^- ds \right) \\ &\quad + \int_{\Gamma_{\mathcal{I}} \cup \Gamma_D} \left( - \{a(\xi) \nabla v\} \cdot \llbracket w \rrbracket - \llbracket v \rrbracket \cdot \{a(\xi) \nabla w\} + \vartheta(\xi) \llbracket v \rrbracket \cdot \llbracket w \rrbracket \right) ds \\ \mathcal{L}_{h,p}(v; \xi) &\equiv \int_{\Omega} f(\xi) v dx - \sum_{\kappa \in \mathcal{T}_h} \int_{\partial_- \kappa \cap \Gamma} n \cdot b(\xi) g_D(\xi) v^+ ds \\ &\quad - \int_{\Gamma_D} g_D(\xi) (n \cdot a(\xi) \nabla v^+ + \vartheta v^+) ds + \int_{\Gamma_N} g_N(\xi) v^+ ds. \end{aligned}$$

The expression above uses the standard notations from the DG literature, but we here provide a brief review for completeness; we refer to [5, 36, 34] for more detailed presentation. We denote by  $\Gamma_{\mathcal{I}}$  the union of all interior facets of  $\mathcal{T}_h$ . We denote by  $\kappa^+$  and  $\kappa^-$  the two elements on an interior facet. The averaging operator on an interior facet is given by  $\{v\} = (v^+ + v^-)/2$ , where  $v^\pm$  are the states evaluated on the boundary of  $\kappa^\pm$  associated with the facet; the averaging operator simplifies to  $\{v\} = v$  on a boundary of  $\Gamma$  of  $\Omega$ . The jump operator on an interior facet is given by  $\llbracket v \rrbracket = v^+ n_{\kappa^+} + v^- n_{\kappa^-}$ , where  $n_{\kappa^\pm}$  the outward-pointing normal on  $\kappa^\pm$ ; the jump operator simplifies to  $\llbracket v \rrbracket = v n$ , where  $n$  is the outward-pointing normal on  $\Gamma$ , on boundary of  $\Omega$ . In addition,  $\partial_- \kappa$  and  $\partial_+ \kappa$  denotes the inflow and outflow part of the element boundary, respectively. Finally,  $\vartheta$  is the discontinuity-penalization parameter. We again refer to [36, 34] for more detailed presentation.

The stochastic DG approximation is as follows: find  $u_{h,p,s} \in \mathcal{V}_{h,p,s}$  such that

$$\mathcal{B}_{h,p,s}(u_{h,p,s}, v_{h,p,s}) = \mathcal{L}_{h,p,s}(v_{h,p,s}) \quad \forall v_{h,p,s} \in \mathcal{V}_{h,p,s},$$

where

$$\begin{aligned} \mathcal{B}_{h,p,s}(w, v) &\equiv \int_{\Xi} \mathcal{B}_{h,p}(w(\cdot, \xi), v(\cdot, \xi); \xi) d\mathbb{P}_\xi, \\ \mathcal{L}_{h,p,s}(v) &\equiv \int_{\Xi} \mathcal{L}_{h,p}(v(\cdot, \xi); \xi) d\mathbb{P}_\xi. \end{aligned}$$

We also introduce a linear output functional of the form  $\mathcal{L}_{h,p,s}^o(u) = \int_{\Xi} \mathcal{L}_{h,p}^o(u(\xi); \xi) d\mathbb{P}_{\xi}$  and the associated adjoint problem: find  $z \in H^2(\mathcal{T}_h) \otimes L^2(\Xi)$  such that

$$\mathcal{B}_{h,p,s}(w, z) = \mathcal{L}_{h,p,s}^o(w) \quad \forall w \in H^2(\mathcal{T}_h) \otimes L^2(\Xi),$$

where  $H^2(\mathcal{T}_h) \equiv \{v \in L^2(\Omega) \mid v|_{\kappa} \in H^2(\kappa), \forall \kappa \in \mathcal{T}_h\}$  is the broken Sobolev space. Our analysis builds on the stability and quasi-optimality of the underlying DG discretization proven by Georgoulis, Hall, Hartmann, and Houston in a series of papers [36, 25, 26, 27, 34]; we in particular leverage the simple relationship between  $\mathcal{B}(\cdot, \cdot)$ ,  $\mathcal{L}(\cdot)$ , and  $\mathcal{J}(\cdot)$  and  $\mathcal{B}(\cdot, \cdot; \xi)$ ,  $\mathcal{L}(\cdot; \xi)$ , and  $\mathcal{J}(\cdot; \xi)$ , respectively.

We conclude this section with a few limitations of the study. We first make two assumptions that are also made in the analysis of (deterministic) DG methods in [36, 34]: (i) the advection field satisfies  $b \cdot \nabla v \in \mathcal{V}_{h,p,s} \quad \forall v \in \mathcal{V}_{h,p,s}$ ; (ii) the diffusion field  $a(\xi)$  is constant over each element. In addition, unlike the analysis in [34], we assume that all elements can be determined via affine transformations.

### 3.2. Approximation theory in spatio-stochastic spaces

We now analyze the approximation properties of the spatio-stochastic approximation space  $\mathcal{V}_{h,p,s}$ . To begin, we first introduce a few quantities that characterize a given (physical) mesh as defined in [34]:

**Definition 2.** Let  $\hat{\kappa} \equiv (0, 1)^d$  be a reference element with the associated coordinate system  $\hat{x} = (\hat{x}_1, \dots, \hat{x}_d)$ . We denote the Jacobian of the mapping from the reference element  $\hat{\kappa}$  to the physical element  $\kappa \in \mathcal{T}_h$  by  $J^{\kappa} : \hat{\kappa} \rightarrow \kappa$ ; note that  $(J^{\kappa})_{i,j} = \frac{\partial x_i}{\partial \hat{x}_j}$ ,  $i, j = 1, \dots, d$ . The singular values of the Jacobian are  $\sigma_1^{\kappa} \geq \dots \geq \sigma_d^{\kappa}$ .

We now analyze the approximation properties of the spatio-stochastic  $L^2$  projection operator  $\Pi_{h,p,s} : H^1(\Omega) \otimes L^2(\Xi) \rightarrow \mathcal{V}_{h,p,s}$ , which satisfies

$$(w - \Pi_{h,p,s} w, v)_{L^2(\Omega \times \Xi)} = 0 \quad \forall v \in \mathcal{V}_{h,p,s}.$$

The ‘‘best-fit’’ projection plays an important role in the *a priori* error analysis of the spatio-stochastic DG method. In particular, as the DG method involves integration of the functions in elements as well as on facets, we require projection error bounds for functions evaluated on both entities. We now state the main result, which is an extension of the result for (deterministic) DG spaces in [25, 26, 34] to spatio-stochastic DG spaces:

**Proposition 3.** For a smooth function  $v : \kappa \times \Xi \rightarrow \mathbb{R}$ , there exists  $C < \infty$  that depends only on the physical dimension  $d$ , stochastic dimension  $P$ , and the physical polynomial degree  $p^{\kappa}$  such that the  $L^2$  and  $H^1$  errors on an element  $\kappa$  and a facet  $f \subset \partial\kappa$  are bounded by

$$\|v - \Pi_{h,p,s} v\|_{L^2(\kappa \times \Xi)} \leq C (F_{h,p}^{\kappa}(v) + F_s^{\kappa}(v)) \quad (8)$$

$$\|\nabla(v - \Pi_{h,p,s} v)\|_{L^2(\kappa \times \Xi)} \leq C (|\sigma_d^{\kappa}|^{-1} F_{h,p}^{\kappa}(v) + F_s^{\kappa}(\nabla v)) \quad (9)$$

$$\|v - \Pi_{h,p,s} v\|_{L^2(f \times \Xi)} \leq C \frac{|f|^{1/2}}{|\kappa|^{1/2}} (F_{h,p}^{\kappa}(v) + F_s^{\kappa}(v) + \sigma_1^{\kappa} F_s^{\kappa}(\nabla v)) \quad (10)$$

$$\|\nabla(v - \Pi_{h,p,s} v)\|_{L^2(f \times \Xi)} \leq C \frac{|f|^{1/2}}{|\kappa|^{1/2}} (|\sigma_d^{\kappa}|^{-1} F_{h,p}^{\kappa}(v) + F_s^{\kappa}(\nabla v) + \sigma_1^{\kappa} F_s^{\kappa}(\nabla^2 v)), \quad (11)$$

where  $|\kappa|$  is the measure (i.e., volume) of element  $\kappa$ ,  $|f|$  is the measure (i.e.,  $d-1$  volume) of facet  $f$ ,  $\sigma_d^\kappa$  is the  $d$ -th singular value of the Jacobian as defined in Definition 2, and

$$F_{h,p}^\kappa(v) \equiv \|D^{\kappa,p+1}(v)\|_{L^2(\kappa \times \Xi)} \equiv \left\| \sum_{j_1=1}^d \cdots \sum_{j_{p+1}=1}^d J_{j_1, i_1}^\kappa \cdots J_{j_{p+1}, i_{p+1}}^\kappa \frac{\partial^{p+1} v}{\partial x_{j_1} \cdots \partial x_{j_{p+1}}} \right\|_{L^2(\kappa \times \Xi)},$$

$$F_s^\kappa(v) \equiv \left[ \sum_{j=1}^P \frac{1}{(2s_j^\kappa)!(s_j^\kappa)^2 2^{2(s_j^\kappa+1)}} \|\partial_{\xi_j}^{s_j^\kappa+1} v\|_{L^2(\kappa \times \Xi)}^2 \right]^{1/2}.$$

*Proof.* The result is an extension of Theorem 5.20 in [34] for deterministic DG spaces to spatio-stochastic DG spaces. The proof is provided in Appendix A.  $\square$

**Remark 4.** In the same setting as Proposition 3, we may appeal to Stirling's formula to obtain a simplified bound for the stochastic error term  $F_s^\kappa(v)$ ,

$$F_s^\kappa(v) \approx \left[ \sum_{j=1}^P C_{s_j^\kappa} s^{-2(s_j^\kappa+1)} \|\partial_{\xi_j}^{s_j^\kappa+1} v\|_{L^2(\kappa \times \Xi)}^2 \right]^{1/2},$$

where  $C_{s_j^\kappa}$  depends only weakly on  $s^\kappa$  compared with the dominant terms in the inequality. This is the typical spectral convergence result for polynomial-degree refinement.

**Remark 5.** If the element is nearly isotropic with a diameter  $h$ , then  $\sigma_d^\kappa \approx \sigma_1^\kappa \equiv h$ , and the spatial error term  $F_{h,p}^\kappa(v)$  simplifies to

$$F_{h,p}^\kappa(v) \approx h^{p+1} \|\nabla^{p+1} v\|_{L^2(\kappa \times \Xi)}.$$

We hence obtain the well-known relationships for the physical space error: e.g.,  $\|v - \Pi_{h,p,s} v\|_{L^2(\kappa \times \Xi)} \leq Ch^{p+1} \|\nabla^{p+1} v\|_{L^2(\kappa \times \Xi)}$ .

In Proposition 3, the error in the spatio-stochastic approximation is decomposed into two pieces: the first is the spatial error  $F_{h,p}^\kappa(\cdot)$ , which depends on the (anisotropic) element size encoded in the mesh Jacobian  $J^\kappa$  and the polynomial degree  $p$ ; the second is the stochastic error  $F_s^\kappa(\cdot)$ , which depends on the anisotropic stochastic expansion degree  $s^\kappa = (s_1^\kappa, \dots, s_P^\kappa)$ . Additionally for the physical error term, we see that the error converges algebraically with respect to  $h^\kappa$  as  $(h^\kappa)^{p^\kappa+1}$ . This expression once again demonstrates the advantage of high-order discretizations. Likewise for the stochastic term we see a spectral convergence in the error with respect to the polynomial chaos expansion order  $s^\kappa$ , again assuming the solution is sufficiently regular. Alluding to our previously mentioned objectives, we see that *both* the spatial and stochastic error must be controlled in order to obtain a truly accurate solution. Otherwise, adapting in one space may be futile if the error is dominated by the opposing term.

### 3.3. A priori error analysis of the stochastic DG method

We now provide the stability analysis and *a priori* error analysis of the spatio-stochastic DG method. To begin, we define the stochastic DG norm:

$$\begin{aligned} \|v\|_{\mathcal{V}_{h,p,s}}^2 &\equiv \sum_{\kappa \in \mathcal{T}_h} \left( \|\sqrt{a}\nabla v\|_{L^2(\kappa \times \Xi)}^2 + \|c_0 v\|_{L^2(\kappa \times \Xi)}^2 \right. \\ &\quad + \frac{1}{2} \| |b \cdot n| v^+ \|_{L^2((\partial\kappa \cap \Gamma) \times \Xi)}^2 + \frac{1}{2} \| |b \cdot n| (v^+ - v^-) \|_{L^2((\partial_- \kappa \setminus \Gamma) \times \Xi)}^2 \\ &\quad \left. + \|\vartheta^{-1/2} \{a \nabla v\}\|_{L^2((\partial\kappa \setminus \Gamma_N) \times \Xi)}^2 + \|\vartheta^{1/2} [v]\|_{L^2((\partial\kappa \setminus \Gamma_N) \times \Xi)}^2 \right); \end{aligned}$$

this is an extension of the DG norm in [36, 34] to stochastic problems by  $\|v\|_{\mathcal{V}_{h,p,s}} \equiv \int_{\Xi} \|v(\cdot, \xi)\|_{\mathcal{V}_{h,p}} d\mathbb{P}_{\xi}$ . The following lemma states the stability of the stochastic DG method:

**Proposition 6** (stability of stochastic DG method). *The stochastic DG method applied to the stochastic advection-diffusion-reaction equation is stable in the sense that*

$$\alpha \|v_{h,p,s}\|_{\mathcal{V}_{h,p,s}}^2 \leq \mathcal{B}_{h,p,s}(v_{h,p,s}, v_{h,p,s}) \quad \forall v_{h,p,s} \in \mathcal{V}_{h,p,s},$$

where  $\alpha$  depends only on the physical dimension  $d$  and the polynomial degree  $p$ .

*Proof.* Theorem 5.6 of [34] states that there exists  $\alpha$  that depends only on the physical dimension  $d$  and the polynomial degree  $p$  such that

$$\alpha \|v_{h,p}\|_{\mathcal{V}_{h,p}}^2 \leq \mathcal{B}_{h,p}(v_{h,p}, v_{h,p}; \xi) \quad \forall v_{h,p} \in \mathcal{V}_{h,p}.$$

The integration of the equation over the stochastic space  $\Xi$  yields

$$\alpha \|v\|_{\mathcal{V}_{h,p,s}}^2 = \alpha \int_{\Xi} \|v(\cdot, \xi)\|_{\mathcal{V}_{h,p}}^2 d\mathbb{P}_{\xi} \leq \int_{\Xi} \mathcal{B}_{h,p}(v(\cdot, \xi), v(\cdot, \xi); \xi) d\mathbb{P}_{\xi} = \mathcal{B}_{h,p,s}(v, v) \quad \forall v \in \mathcal{V}_{h,p,s},$$

where we have appealed to the definition of  $\|\cdot\|_{\mathcal{V}_{h,p,s}}$  and  $\mathcal{B}(\cdot, \cdot)$ .  $\square$

In words, the stochastic DG method is coercive with respect to the stochastic DG norm. We next state the main theorem of this section: the *a priori* analysis for the output error.

**Proposition 7.** *The output error in the stochastic DG method applied to the stochastic advection-diffusion-reaction equation is bounded by*

$$|\mathcal{J}(u) - \mathcal{J}_{h,p,s}(u_{h,p,s})|^2 \leq C \sum_{\kappa \in \mathcal{T}_h} (\tilde{e}_{\text{pr}}^{\kappa}) \sum_{\kappa \in \mathcal{T}_h} (\tilde{e}_{\text{du}}^{\kappa}),$$

where  $\beta_1 \equiv \|c + \nabla \cdot b\|_{L^\infty(\kappa \times \Xi)}$ ,  $\beta_2 \equiv \|b\|_{L^\infty(\kappa \times \Xi)}$ ,  $\gamma_1 \equiv \|c/c_0\|_{L^\infty(\kappa \times \Xi)}^2$ ,  $\gamma_2 \equiv \|(c + \nabla \cdot b)/c_0\|_{L^\infty(\kappa \times \Xi)}^2$ , and

$$\begin{aligned} \tilde{e}_{\text{pr}}^{\kappa} &\equiv \left( \frac{a}{(\sigma_d^{\kappa})^2} + \frac{\beta_2}{\sigma_d^{\kappa}} + (\beta_1 + \gamma_1) \right) (E_{h,p}^{\kappa}(u)^2 + E_s^{\kappa}(u)^2) \\ \tilde{e}_{\text{du}}^{\kappa} &\equiv \left( \frac{a}{(\sigma_d^{\kappa})^2} + \frac{\beta_2}{\sigma_d^{\kappa}} + (\beta_1 + \gamma_2) \right) (E_{h,p}^{\kappa}(z)^2 + E_s^{\kappa}(z)^2); \end{aligned}$$

here,

$$\begin{aligned} E_{h,p}^\kappa(v) &\equiv F_{h,p}^\kappa(v), \\ E_s^\kappa(v) &\equiv F_s^\kappa(v)^2 + ((\sigma_1^\kappa)^2 + (\sigma_d^\kappa)^2)F_s^\kappa(\nabla v)^2 + (\sigma_1^\kappa)^2(\sigma_d^\kappa)^2F_s^\kappa(\nabla^2 v)^2, \end{aligned}$$

where  $F_{h,p}^\kappa(\cdot)$  and  $F_s^\kappa(\cdot)$  are defined in Proposition 3, and  $\sigma_1^\kappa$  and  $\sigma_d^\kappa$  are defined in Definition 2.

*Proof.* The result is an extension of Theorem 5.23 in [34] for deterministic DG methods to our spatio-stochastic DG methods. The proof is provided in Appendix A.  $\square$

We summarize interpretations of the proposition in the following remark:

**Remark 8.** Proposition 7 provides the following interpretations:

- (i) *The stochastic DG approximation inherits the stability of the underlying DG method for the advection-diffusion-reaction equation. In words, as long as we provide an approximation space  $\mathcal{V}_{h,p,s}$  in which the primal solution  $u_{h,p,s}$  and the adjoint  $z_{h,p,s}$  are well approximated in the sense  $u - \Pi_{h,p,s}u$  and  $z - \Pi_{h,p,s}z$  are small, the stochastic DG method will provide an accurate output prediction.*
- (ii) *We must control both the error in the physical space  $E_{h,p}^\kappa(\cdot)$  and the error in the stochastic space  $E_s^\kappa(\cdot)$  to provide an accurate output prediction. As discussed in Section 3.2, the former depends on the choice of the (anisotropic) element size  $h^\kappa$  and the polynomial degree  $p$ , and the latter depends on the choice of the (anisotropic) stochastic polynomial degree distribution  $s^\kappa$ .*
- (iii) *The output error depends on the errors in both the primal solution  $u$  and the adjoint solution  $z$ . To equidistribute the error, an effective goal-oriented spatio-stochastic adaptive algorithm must judiciously control the anisotropic element size  $\{h^\kappa\}_{\kappa \in \mathcal{T}_h}$  and anisotropic stochastic polynomial degrees  $\{s^\kappa \equiv (s_1^\kappa, \dots, s_p^\kappa)\}_{\kappa \in \mathcal{T}_h}$  depending on the local spatio-stochastic behavior of the primal and dual solutions.*

## 4. Error Estimation and Spatio-Stochastic Adaptation

We now provide an overview of the error estimation and adaptation techniques used in this work. Our goal is twofold: (i) to estimate the error  $\mathcal{E} \equiv \mathcal{J} - \mathcal{J}_{h,p,s}(u_{h,p,s})$  in order to gauge the quality of our overall approximation, while accounting for the error due to both spatial and stochastic approximations; (ii) to adaptively identify a sequence of spatio-stochastic approximation spaces  $\mathcal{V}_{h,p,s}$  that minimize the estimate of the error  $\mathcal{E}$  for a given computational cost. Output-based error estimators based on the dual-weighted residual (DWR) method [12] have been shown to be effective for deterministic aerodynamics problems [24, 34]; here we will use the DWR method to estimate the spatio-stochastic error and find an anisotropic spatio-stochastic refinement sequence to control the error.

### 4.1. Spatio-stochastic error estimation

As the name implies, the DWR method estimates the error in an output by weighting the residual by the dual (or adjoint) solution. The dual solution identifies the regions in the domain where the output is most sensitive to changes in the residual. To this end, we note that the standard

definition of an adjoint problem [12] can be stated for our problem as: find  $\bar{z} \in \mathcal{V}_{h,p,s} + (H^1(\Omega) \otimes L^2(\Xi))$  such that

$$\overline{\mathcal{R}}'_{h,p,s}[u, u_{h,p,s}](w, \bar{z}) = \overline{\mathcal{J}}'_{h,p,s}[u, u_{h,p,s}](w) \quad \forall w \in \mathcal{V}_{h,p,s} + (H^1(\Omega) \otimes L^2(\Xi));$$

here  $\overline{\mathcal{R}}'_{h,p,s}[u, u_{h,p,s}](w, z)$  and  $\overline{\mathcal{J}}'_{h,p,s}[u, u_{h,p,s}](w)$  are the mean-value linearized Fréchet derivative of the residual and output given by  $\overline{\mathcal{R}}'_{h,p,s}[u, u_{h,p,s}](w, z) = \int_{\theta=0}^1 \mathcal{R}'_{h,p,s}(\theta u + (1-\theta)u_{h,p,s}; w, z) d\theta$  and  $\overline{\mathcal{J}}'_{h,p,s}[u, u_{h,p,s}](w) = \int_{\theta=0}^1 \mathcal{J}'_{h,p,s}(\theta u + (1-\theta)u_{h,p,s}; w) d\theta$ , where  $\mathcal{R}'_{h,p,s}(\theta u + (1-\theta)u_{h,p,s}; w, z)$  and  $\mathcal{J}'_{h,p,s}(\theta u + (1-\theta)u_{h,p,s}; w)$  are the Fréchet derivative of  $\mathcal{R}_{h,p,s}(\cdot, z)$  and  $\mathcal{J}_{h,p,s}(\cdot)$ , respectively, about  $\theta u + (1-\theta)u_{h,p,s}$  in the direction  $w$ . Using the mean-value linearized adjoint, the output error can be expressed as

$$\mathcal{E} = \mathcal{J} - \mathcal{J}_{h,p,s}(u_{h,p,s}) = -\mathcal{R}_{h,p,s}(u_{h,p,s}, \bar{z}).$$

However, the mean-value linearized adjoint is not computable in practice because (i) it requires the solution in an infinite dimensional space  $\mathcal{V}_{h,p,s} + (H^1(\Omega) \otimes L^2(\Xi))$  and (ii) it requires exact mean-value linearization.

To obtain a computable error estimate, we (i) seek a solution and output in an enriched finite dimensional space  $\mathcal{V}_{h,\hat{p},\hat{s}} \supset \mathcal{V}_{h,p,s}$  and (ii) linearize the adjoint problem about  $u_{h,p,s} \in \mathcal{V}_{h,p,s}$ . This is a direct extension of commonly used approximations for the standard deterministic DWR method [12, 24, 34] to spatio-stochastic problems. To this end, we first introduce

$$\mathcal{V}_{h,\hat{p},\hat{s}} \equiv \{v \in L^2(\Omega \times \Xi)^m \mid v|_{\kappa} \in (\mathcal{P}^{\hat{p}^\kappa}(\kappa) \otimes \mathcal{P}^{\hat{s}^\kappa}(\Xi))^m, \forall \kappa \in \mathcal{T}_h\}, \quad (12)$$

where  $\hat{p}^\kappa = p^\kappa + 1$  and  $\hat{s}^\kappa = (\hat{s}_1^\kappa, \dots, \hat{s}_P^\kappa) = (s_1^\kappa + 1, \dots, s_P^\kappa + 1) = s^\kappa + 1$  for all  $\kappa \in \mathcal{T}_h$ . We then solve the approximate dual problem: find  $z_{h,\hat{p},\hat{s}} \in \mathcal{V}_{h,\hat{p},\hat{s}}$  such that

$$\mathcal{R}'_{h,p,s}(u_{h,p,s}; w_{h,\hat{p},\hat{s}}, z_{h,\hat{p},\hat{s}}) = -\mathcal{J}'_{h,p,s}(u_{h,p,s}; w_{h,\hat{p},\hat{s}}) \quad \forall w_{h,\hat{p},\hat{s}} \in \mathcal{V}_{h,\hat{p},\hat{s}}. \quad (13)$$

Our spatio-stochastic error estimate is then given by

$$\mathcal{E} \approx \mathcal{E}_{h,p,s} \equiv \mathcal{R}_{h,p,s}(u_{h,p,s}, z_{h,\hat{p},\hat{s}}). \quad (14)$$

To drive adaptive mesh refinement, we also introduce the element-wise localized error indicator:

$$\eta_\kappa \equiv |\mathcal{R}_{h,p,s}(u_{h,p,s}, z_{h,\hat{p},\hat{s}}|_\kappa)| \quad \forall \kappa \in \mathcal{T}_h; \quad (15)$$

the error indicator is simply the element-wise restriction of the (global) error estimate (14). Because Galerkin orthogonality holds element-wise for DG, and by extension SDG, methods, the element-wise error indicator can also be expressed as  $\eta_\kappa \equiv |\mathcal{R}_{h,p,s}(u_{h,p,s}, z_{h,\hat{p},\hat{s}}|_\kappa)| = |\mathcal{R}_{h,p,s}(u_{h,p,s}, (z_{h,\hat{p},\hat{s}} - \Pi_{h,p,s} z_{h,\hat{p},\hat{s}})|_\kappa)|$ . In other words, thanks to element-wise Galerkin orthogonality, the subtraction of  $\Pi_{h,p,s} z_{h,\hat{p},\hat{s}}$  is implicit in DG methods; this is unlike continuous Galerkin methods which require explicit subtraction to achieve effective error localization.

We emphasize that the formulation is a straightforward extension of the existing DWR error estimation for deterministic PDEs to SPDEs where the stochastic behavior is approximated using an enriched PC expansion. Just as the physical polynomial degree is increased for the deterministic DWR method, so too is the stochastic degree increased in the stochastic framework.

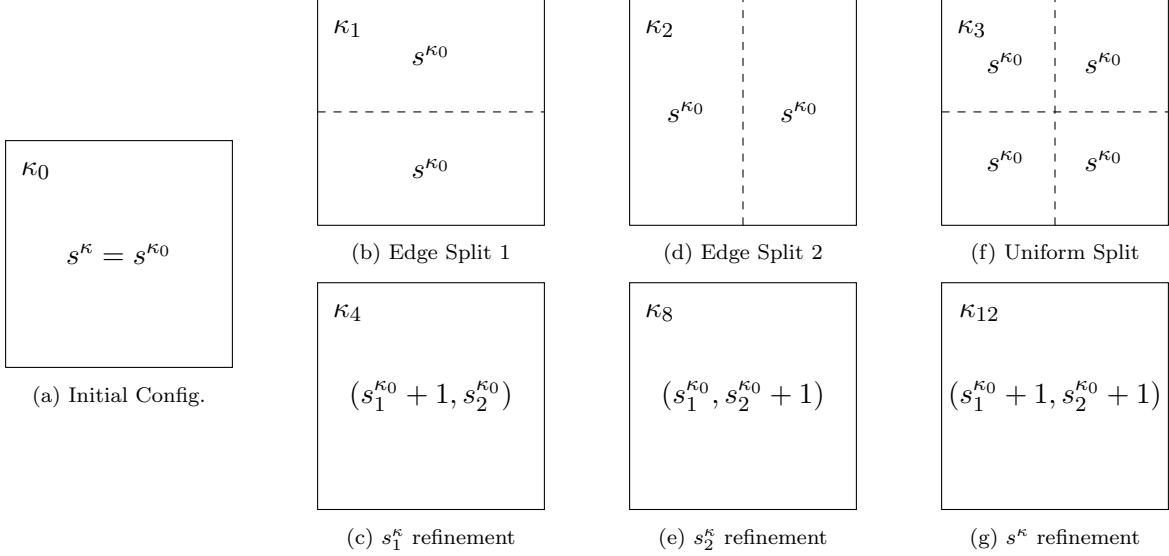


Figure 1: Possible refinement configurations given a two-dimensional spatial domain with two stochastic parameters.

#### 4.2. Spatio-stochastic anisotropic error estimation and adaptation

We now present our spatio-stochastic anisotropic adaptation strategy. In this work, we consider anisotropic  $h$  refinement in the  $d$ -dimensional physical space and anisotropic  $s$  refinement in the  $P$ -dimensional stochastic space. To exploit the full potential of the flexible stochastic DG method presented in Section 2, we must answer the following two questions: (i) *which* elements should be refined; (ii) *how* to best refine these elements.

For (i) we select some fraction of elements with the largest error indicators  $\eta_\kappa$  given by (15) for refinement. Since it is generally not possible to know *a priori* whether a specific refinement fraction may be too small and induce excessive refinement iterations, or too large and inefficiently over-refine the domain, a heuristic value between 10% and 20% is often used [24]. For (ii), we must first decide whether to refine in the physical space by splitting elements into multiple children, to refine in the stochastic space by increasing the PC expansion degree, or to do both. For physical-space refinement, we have the option to split our element in any combination of reference coordinate directions  $x_1, \dots, x_d$  in an anisotropic manner. Likewise, for stochastic-space refinement, we have the option to increase the PC expansion degree in any combination of the stochastic dimensions  $\xi_1, \dots, \xi_P$  in a similarly anisotropic manner. We note the word “anisotropic” in our context refers to anisotropy both in deciding physical or stochastic refinement and in exploiting anisotropy within  $d$ -dimensional physical and/or  $P$ -dimensional stochastic spaces. A concrete example of refinement options for a square element in  $d \equiv 2$  spatial dimension and  $P \equiv 2$  stochastic dimension is shown in Figure 1; there are a total of  $n_{\text{config}} = 16$  potential spatio-stochastic anisotropic refinement options in this case, including the option to perform no refinement at all.

While the elemental indicator  $\eta_\kappa$  given by (15) provides sufficient information for element marking (i.e., step (i)), it does not provide the directional information required to make spatio-stochastic anisotropic refinement decision (i.e., step (ii)). In order to select which option will most efficiently reduce the error on each element, we estimate the error reduction associated with each refinement option using a local solver, which is a popular strategy for anisotropic adaptation for (deterministic) DG methods [27, 34, 17, 62]. One approach is to construct anisotropic error estimates based on

local solutions on each of the candidate refinement spaces

$$\mathcal{V}_{h,p,s^{\kappa_i}}^{\kappa_i} \equiv \bigoplus_{\kappa_i} (\mathcal{P}^{\mathcal{P}^{\kappa_i}}(\kappa_i) \otimes \mathcal{P}^{s^{\kappa_i}}(\Xi))^m,$$

where each configuration option is uniquely characterized by each  $\kappa_i$  and  $s^{\kappa_i}$ , for each of  $i = 1, \dots, n_{\text{config}}$  options. However, due to the exponential dependence of the number of refinement configurations on the physical and stochastic dimension of the problem, the use of a local solver quickly becomes intractable for higher dimensional problems. To mitigate this, we introduce a projection based replacement, where the adjoint is projected down into the primal space for each configuration.

To this end, we first introduce a locally refined approximation space

$$\mathcal{V}_{h,\hat{p},\hat{s}}^{\kappa} \equiv (\mathcal{P}^{\hat{p}^{\kappa}}(\kappa) \otimes \mathcal{P}^{\hat{s}^{\kappa}}(\Xi))^m,$$

where  $\hat{p}^{\kappa} = p^{\kappa} + 1$  and  $\hat{s}^{\kappa} = (\hat{s}_1^{\kappa}, \dots, \hat{s}_P^{\kappa}) = (s_1^{\kappa} + 2, \dots, s_P^{\kappa} + 2) = s^{\kappa} + 2$ . In words, the space is one degree enriched in the physical space and two degrees enriched in the stochastic space. We then consider a locally refined dual problem: find  $z_{h,\hat{p},\hat{s}}^{\kappa} \in \mathcal{V}_{h,\hat{p},\hat{s}}^{\kappa}$  such that

$$\mathcal{R}_{h,\hat{p},\hat{s}}^{\kappa}(u_{h,p,s}; w_{h,\hat{p},\hat{s}}, z_{h,\hat{p},\hat{s}}^{\kappa}) = \mathcal{J}_{h,\hat{p},\hat{s}}^{\kappa}(u_{h,p,s}; w_{h,\hat{p},\hat{s}}) \quad \forall w_{h,\hat{p},\hat{s}} \in \mathcal{V}_{h,\hat{p},\hat{s}}^{\kappa}. \quad (16)$$

For each element-wise local solve, the states on neighboring elements are held constant and treated as boundary conditions. We next introduce an approximation space associated with the refinement option  $i \in \{1, \dots, n_{\text{config}}\}$  :

$$\mathcal{V}_{h,\hat{p},\hat{s}^{\kappa_i}}^{\kappa_i} \equiv \bigoplus_{\kappa_i} (\mathcal{P}^{\hat{p}^{\kappa_i}}(\kappa_i) \otimes \mathcal{P}^{\hat{s}^{\kappa_i}}(\Xi))^m,$$

where  $\{\kappa_i\}$  is the set of sub-elements that results from  $h$ -refinement in physical space, and  $\hat{s}^{\kappa_i} = (\hat{s}_1^{\kappa_i}, \dots, \hat{s}_P^{\kappa_i})$  is the multi-index of anisotropic polynomial degrees that results from  $s$ -refinement in stochastic space. We then project the enriched dual solution onto refinement option  $i \in \{1, \dots, n_{\text{config}}\}$ : find  $z_{h,\hat{p},\hat{s}^{\kappa_i}}^{\kappa_i} \equiv \Pi_{h,\hat{p},\hat{s}^{\kappa_i}}^{\kappa_i} z_{h,\hat{p},\hat{s}}^{\kappa_i} \in \mathcal{V}_{h,\hat{p},\hat{s}^{\kappa_i}}^{\kappa_i}$  such that

$$(z_{h,\hat{p},\hat{s}}^{\kappa_i} - z_{h,\hat{p},\hat{s}^{\kappa_i}}^{\kappa_i}, w_{h,p,s^{\kappa_i}}) = 0 \quad \forall w_{h,p,s^{\kappa_i}} \in \mathcal{V}_{h,\hat{p},\hat{s}^{\kappa_i}}^{\kappa_i}.$$

Thereby enabling the computation of the element-wise error estimate

$$\eta_{\kappa_i} \equiv |\mathcal{R}_{h,p,s}(u_{h,p,s}, z_{h,\hat{p},\hat{s}^{\kappa_i}}^{\kappa_i})|, \quad i \in \{1, \dots, n_{\text{config}}\}. \quad (17)$$

Based on the localized error estimates  $\{\eta_{\kappa_i}\}_{i=1}^{n_{\text{config}}}$ , we determine which refinement configuration yields the most efficient error reduction. Specifically, we choose the configuration that maximizes the ratio of error reduction to increase in degrees of freedom, i.e.

$$i^* \equiv \max_{i=1, \dots, n_{\text{config}}} \frac{|\eta_{\kappa_i}|/|\eta_{\kappa_0}|}{|\text{dof}_{\kappa_i}|/|\text{dof}_{\kappa_0}|}. \quad (18)$$

For a problem with two spatial and stochastic dimensions,  $n_{\text{config}} = 16$ , and the algorithm may choose between any combination of the configurations shown in Figure 1. The goal-oriented spatio-stochastic adaptation algorithm described in this section is summarized in Algorithm 2.

---

**Algorithm 2** Goal-oriented spatio-stochastic adaptation.

---

**Input:**Initial mesh:  $\mathcal{T}_h$ Physical polynomial degree:  $\{p^\kappa\}_{\kappa \in \mathcal{T}_h}$ Initial stochastic polynomial degree  $\{s^\kappa = (s_1^\kappa, \dots, s_P^\kappa)\}_{\kappa \in \mathcal{T}_h}$ Error tolerance:  $\mathcal{E}_{\text{tol}}$ **Output:**Sequence of outputs:  $\{\mathcal{J}_{h,p,s}(u_{h,p,s})\}$ Sequence of error estimates:  $\{\mathcal{E}_{h,p,s}\}$ 

- 1: **while**  $\mathcal{E}_{h,p,s} \geq \mathcal{E}_{\text{tol}}$  **do**
  - 2:     Find state  $u_{h,p,s} \in \mathcal{V}_{h,p,s}$  that satisfies the primal problem (4).
  - 3:     Find adjoint  $z_{h,\hat{p},\hat{s}} \in \mathcal{V}_{h,\hat{p},\hat{s}}$  that satisfies the dual problem (13)
  - 4:     Evaluate the error estimate  $\mathcal{E}_{h,p,s}$  given by (14); terminate if  $\mathcal{E}_{h,p,s} \leq \mathcal{E}_{\text{tol}}$
  - 5:     Evaluate the error indicator  $\{\eta_\kappa\}_{\kappa \in \mathcal{T}_h}$
  - 6:     **for**  $\kappa \in \{\kappa \in \mathcal{T}_h \mid \eta_\kappa \text{ is in top } \sim 15\%\}$  **do**
  - 7:         Find enriched dual solution  $z_{h,\hat{p},\hat{s}} \in \mathcal{V}_{h,\hat{p},\hat{s}}^\kappa$  that satisfies (16)
  - 8:         Evaluate local error estimate  $\{\eta^{\kappa_i}\}_{i=1}^{n_{\text{config}}}$  using (17) for all refinement options.
  - 9:         Choose the optimal refinement index  $i^*$  according to (18).  
          Refine mesh  $\mathcal{T}_h$  and update stochastic polynomial degree  $\{s^\kappa\}_{\kappa \in \mathcal{T}_h}$ .
- 

## 5. Numerical Examples

We consider two numerical examples in this section. The first example is the advection-diffusion equation, which is simple but allows us to study the behavior of the scheme in detail and has been analyzed in Section 3. The second, more engineering-relevant, example is the uncertainty quantification for two cases of transonic turbulent aerodynamic flows over an airfoil.

### 5.1. Advection Diffusion Equation

We consider a stochastic advection-diffusion equation over the  $d = 2$ -dimensional rectangular physical domain  $\Omega \equiv (-1.5, 1.5) \times (0, 1)$  and the  $P = 2$ -dimensional stochastic domain  $\Xi \equiv [1, 50] \times [1, 50]$  given by

$$-\nabla \cdot (a \nabla u) + \nabla \cdot (bu) = 0 \quad \text{a.e. in } \Omega \times \Xi,$$

where  $a \equiv 10^{-3}$  is the fixed diffusivity, and  $b : \Xi \times \Omega \rightarrow \mathbb{R}^2$  is the spatially varying stochastic advection field given by  $b^T = [\xi_0 + x_1 \xi_1, 0]$  for  $\xi_0 \sim \mathcal{U}[1, 50]$  and  $\xi_1 \sim \mathcal{U}[1, 50]$ . The bounds on our stochastic input parameters have been chosen in order to demonstrate anisotropic refinement in the stochastic domain. The boundary conditions are

$$\begin{aligned} -(b \cdot n)u + a \frac{\partial u}{\partial n} &= 0 \quad \text{a.e. on } \{-1.5\} \times (0, 1) \times \Xi, \\ a \frac{\partial u}{\partial n} &= 0 \quad \text{a.e. on } \{1.5\} \times (0, 1) \times \Xi, \\ u &= 1 \quad \text{a.e. on } (-1.5, 1.5) \times \{0\} \times \Xi, \\ u &= 0 \quad \text{a.e. on } (-1.5, 1.5) \times \{1\} \times \Xi, \end{aligned}$$

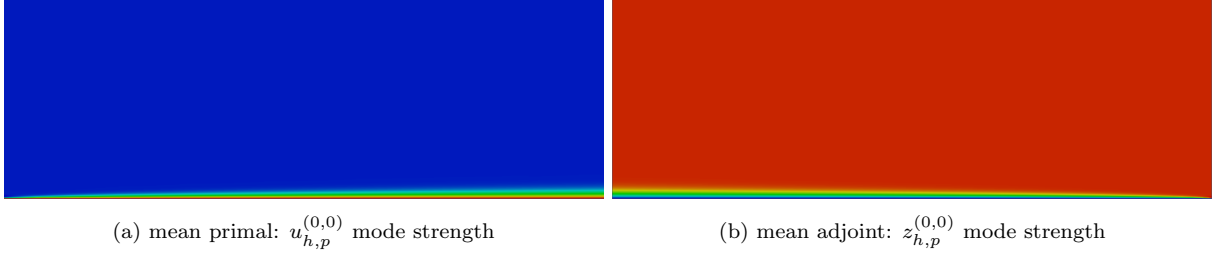


Figure 2: The mean primal and adjoint solutions to the advection-diffusion problem.

where  $n$  is the outward-pointing unit normal on  $\partial\Omega$ . The output functional of interest is the mean of the bottom-boundary diffusion flux,

$$\mathcal{J}(u) \equiv \int_{\Xi} \int_{\Gamma_b} a \frac{\partial u}{\partial n} ds d\mathbb{P}_{\xi} \quad (19)$$

for  $\Gamma_b \equiv (-1.5, 1.5) \times \{0\}$ . We readily obtain the associated adjoint problem following the procedure described in [29, 33]:

$$-b \cdot (\nabla z) - \nabla \cdot (a \nabla z) = 0 \quad \text{a.e. in } \Omega \times \Xi,$$

with the boundary conditions

$$\begin{aligned} a \frac{\partial z}{\partial n} &= 0 \quad \text{a.e. on } \{-1.5\} \times (0, 1) \times \Xi, \\ (b \cdot n)z + a \frac{\partial z}{\partial n} &= 0 \quad \text{a.e. on } \{1.5\} \times (0, 1) \times \Xi, \\ z &= 1 \quad \text{a.e. on } (-1.5, 1.5) \times \{0\} \times \Xi, \\ z &= 0 \quad \text{a.e. on } (-1.5, 1.5) \times \{1\} \times \Xi. \end{aligned}$$

The mean primal and adjoint solutions to the problem are shown in Figure 2. Both the primal and adjoint problems exhibit a thin boundary layer of thickness  $\mathcal{O}(\sqrt{a/|b(\xi)|})$ ; note that this boundary layer thickness depends on  $\xi \in \Xi$ , and is chosen to be thin in order to demonstrate spatio-stochastic localization.

We recall that, in the view of Remark 1, the SDG method yields a set of (sparse) mode strengths; Figure 3 shows some of these sparse mode strengths of the primal solution that capture the stochastic dependence of the problem. We note that the expansions are essentially zero everywhere except in the boundary layer. The localized nature of the mode strength permits the efficient, sparse representation of these fields. We also note that — by construction — higher-order expansion fields have fewer nonzero elements than their lower-order counterparts.

We consider the solution of the advection-diffusion equation using three different refinement strategies:

- (i) *Uniform refinement.* In each refinement iteration, we simply refine all elements into four child elements and increase stochastic polynomial degree by one in all stochastic dimensions.
- (ii) *Isotropic adaptive  $h$ s refinement.* In each refinement iteration, we mark top 15% of the elements with highest error indicator  $\eta_{\kappa}$  for refinement. We then refine each of the marked elements by isotropically splitting it into four child elements and increasing the stochastic

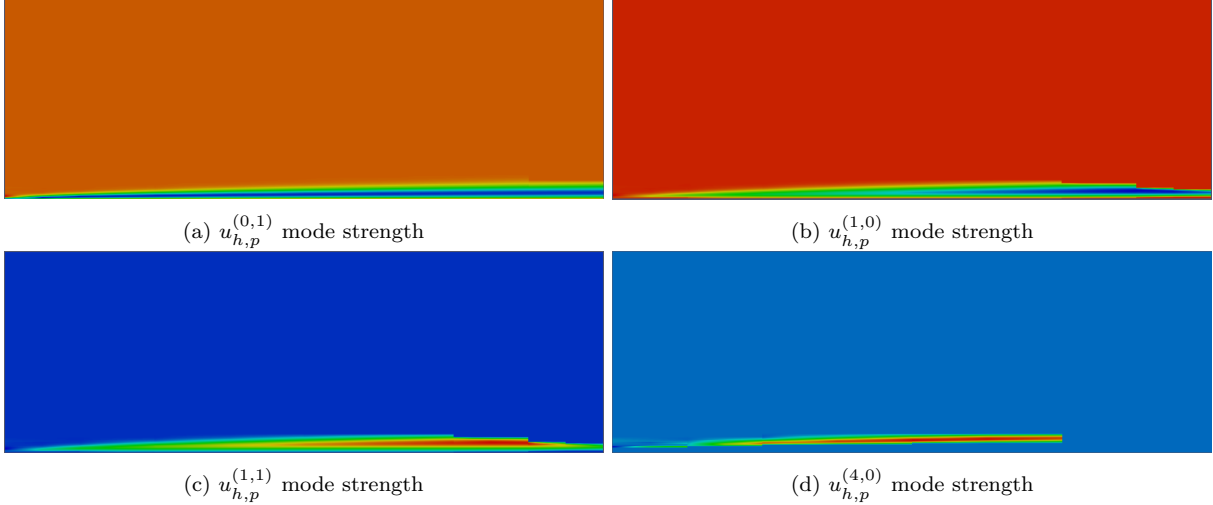


Figure 3: Selected sparse mode strengths of the primal solution to the advection-diffusion problem.

polynomial degree by one in all stochastic dimensions. This refinement exploits the spatio-stochastic structure of the problem and yields a sequence of spaces with a spatially varying physical element size  $h^\kappa$  and stochastic polynomial degree  $s^\kappa$ .

- (iii) *Anisotropic adaptive  $hs$  refinement (Algorithm 2)*. In each refinement iteration, we mark the top 15% of the elements with largest error indicator  $\eta_\kappa$  for refinement. We then refine each element using the “optimal” refinement strategy from  $n_{\text{config}}$  potential options based on the anisotropic error indicators  $\{\eta^{\kappa_i}\}_{i=1}^{n_{\text{config}}}$ . The refinement yields a sequence of spaces with spatially varying *anisotropic*  $h^\kappa$  and  $s^\kappa$  that are chosen “optimally” by Algorithm 2.

Each refinement starts from a mesh consisting of  $12 \times 12$  rectangular elements and an initial stochastic order of  $\{s^\kappa = (0, 0)\}_{\kappa \in \mathcal{T}_h}$ ; i.e. a uniform rectangular mesh with no ability to represent stochastic variation. To the best of our knowledge, both isotropic and anisotropic adaptive  $hs$  refinement algorithms have not been explored in the past.

Figure 4a shows the output convergence of the three refinement strategies. Uniform refinement controls both the physical and stochastic errors and yields a sequence of convergent approximations. The isotropic adaptive  $hs$  refinement achieves a higher “efficiency”, which we characterize by the number of degrees of freedom required to achieve a given error, by localizing the refinement to the boundary layer region. The anisotropic adaptive  $hs$  refinement achieves a further efficiency improvement over the uniform refinement scheme, requiring two orders of magnitude fewer degrees of freedom to achieve an output error of less than  $10^{-3}$ . The reference solution used to calculate the error is computed using a highly refined approximation space resulting from 14 adaptation iterations of the anisotropic refinement strategy, which yields a relative error estimate of  $4 \times 10^{-5}$ . Given the minimum observed effectivity during the final five iterations of  $\approx 0.8$ , we conservatively estimate the true error to be  $6 \times 10^{-5}$  or 1.5 times the estimated error at the reference solution. Hence the refined solution should serve as an accurate reference solution at the computed error levels.

Figure 4a also shows the error estimate  $\mathcal{E}_{h,p,s}$  observed during the refinement iterations. We observe that the error estimate is effective; for nearly every solution evaluation across each refinement method, the error estimate is accurate in comparison with the output error computed against

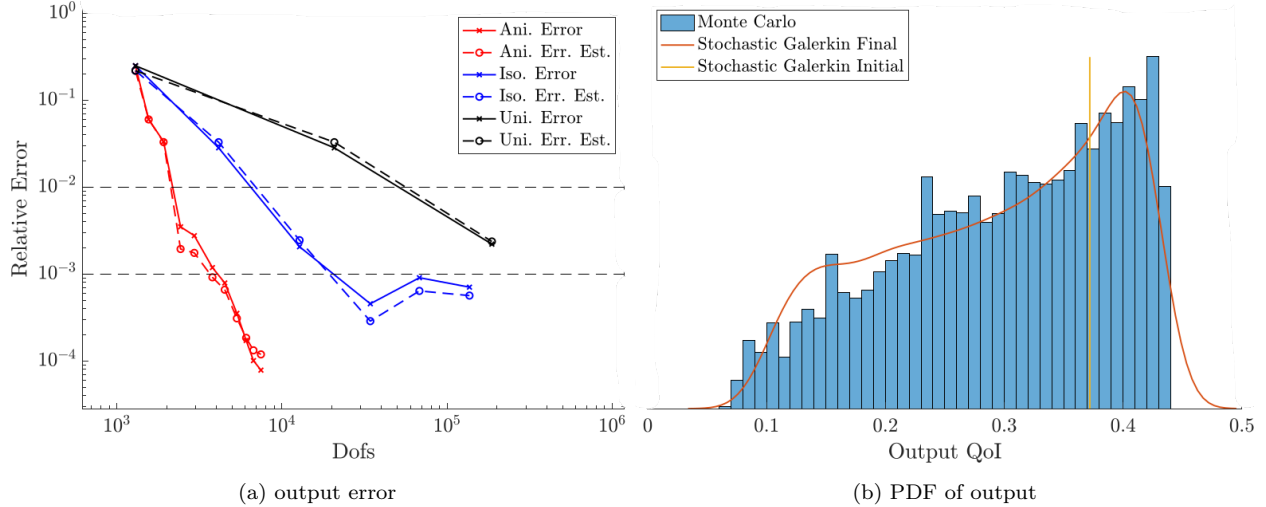


Figure 4: Left: output error convergence of the stochastic DG algorithms applied to the advection-diffusion problem. Right: output distribution obtained using the anisotropic spatio-stochastic DG method in the first and final iterations as well as using Monte-Carlo method.

the heavily refined solution. Hence, our method provides a reliable output error estimate for the SPDE that accounts for both the physical and stochastic approximation error.

In order to further illustrate the accuracy of our spatio-stochastic adaption framework, we also consider how the shape of the output probability density function (PDF) changes as approximation is updated, as well as how it compares against standard Monte Carlo. Figure 4b shows the predicted PDFs for the initial and final iterations of the anisotropic spatio-stochastic adaptive DG method, in comparison with a Monte Carlo simulation consisting of twenty-five thousand samples. At the initial iteration, the prediction is not a PDF but a scalar value, as we have  $\{s^\kappa = (0, 0)\}_{\kappa \in \mathcal{T}_h}$  and we require at least a linear PC expansion to capture parametric variations. We see that the PDF predicted by the final anisotropic refinement iteration is in good agreement with the PDF determined by the Monte Carlo method; however, the spatio-stochastic adaptation scheme requires only  $\mathcal{O}(10)$  (albeit stochastic) DG solves, compared to the  $\mathcal{O}(10,000)$  (deterministic) DG solves required by the Monte Carlo method; we will shortly present a runtime comparison.

Figure 5 shows the mesh and the stochastic polynomial degree field for the final anisotropic adaptive  $hs$  refinement. We see that the algorithm has opted to compute higher-degree mode strengths only along the bottom boundary as expected. In addition, we observe the algorithm chooses to use only linear expansions with respect to  $\xi_2$  while using up to seventh-order expansions for  $\xi_1$ , thereby exploiting the anisotropy in the stochastic domain. We stress the higher-order mode strengths are activated on a given element only if the adaptive algorithm deems it necessary; this enables an efficient, sparse representation of the stochastic dependence of the problem, particularly for cases where this dependence is strongly localized within the spatial domain of the problem.

Table 1 compares the serial runtime breakdown for the anisotropic, isotropic, and Monte Carlo algorithms, each of which reaches a comparable relative error of approximately 0.030%. For the Monte Carlo method, we compute each sample using anisotropic spatially adaptive DG method

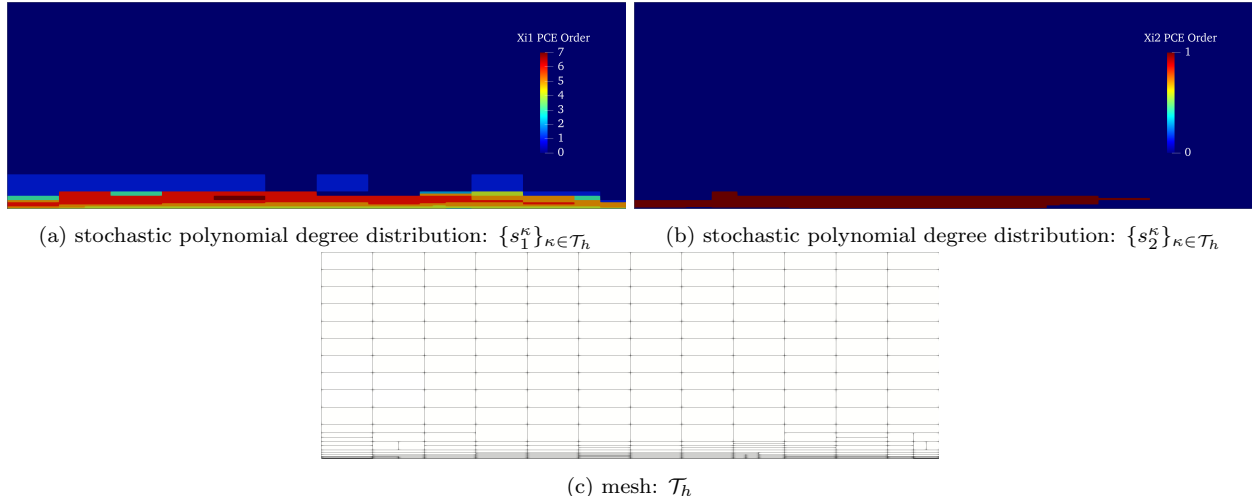


Figure 5: The approximation space  $\mathcal{V}_{h,p,s}$  generated by the anisotropic spatio-stochastic adaptive DG method for the advection-diffusion problem.

	primal solve	adjoint solve	local solves	cumulative
anisotropic adapt	2.7	6.8	21.7	99.7
isotropic adapt	50.3	122.3	-	265.8
Monte Carlo	0.05	0.04	-	$1.4 \times 10^6$

Table 1: Runtime breakdown, normalized against the runtime for a single Monte Carlo sample, to reach the relative error of 0.03%, for the advection-diffusion problem. The first three columns shows the runtime for the final adaptation iteration — i.e., the 7th and 4th iteration for anisotropic and isotropic adaptation respectively — only, while the last column shows the runtime for the entire adaptation process.

to achieve the spatial error estimate of approximately  $0.015\%$ <sup>1</sup> and compute  $1.4 \times 10^6$  samples to achieve the stochastic error of approximately 0.015% such that the combined error is approximately 0.030%. Table 1 shows that the spatio-stochastic methods require significantly less cumulative time to reach the target error level compared to standard Monte Carlo for this low-dimensional problem. We also note that, for this linear problem, the local solves constitutes a significant fraction of the overall runtime for the anisotropic spatio-stochastic method; however, as we will see in our second example, this fraction decreases considerably for large-scale nonlinear problems because (i) the local solve is embarrassingly parallel and perfectly scalable and (ii) the local solve requires a much smaller number of Newton iterations to converge than the (global) primal solve.

Lastly, we demonstrate the importance of combined error estimation and control through the lack of convergence if only one of either spatial or stochastic refinement is used. Figure 6 shows the anisotropic  $h$  (only) refinement for a few different values of fixed (and global)  $s$  degrees. We see that in each case the convergence eventually stagnates; in order to truly capture the correct output, one must estimate and refine with respect to the combined spatio-stochastic error in the solution. This is to say, that without combined error control, the accuracy of spatial or stochastic refinement

<sup>1</sup>The error estimate effectivity observed for a randomly chosen subset of 10 parameter values is  $\approx 0.95$ , and hence we expect the true spatial error to be approximately 0.015% as well.

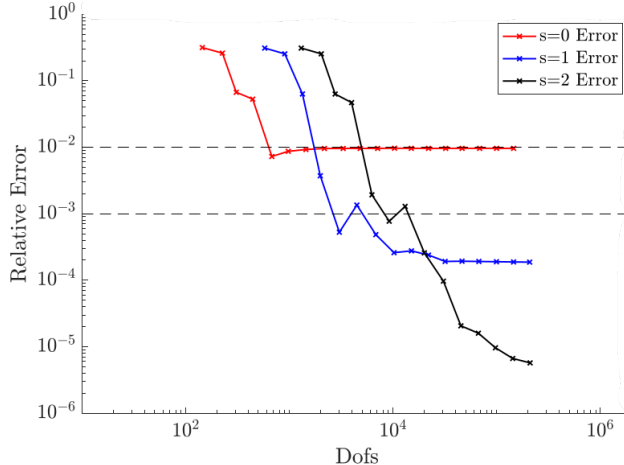


Figure 6: Error stagnation of  $h$ -only refinement for the advection-diffusion problem.

schemes are necessarily limited by the lack of refinement in the opposite domain, as predicted by Theorem 7.

## 5.2. Transonic Reynolds-averaged Navier-Stokes (RANS) flow

For a more practical demonstration of spatio-stochastic adaptivity, we consider a two-dimensional turbulent flow over a RAE 2822 airfoil modeled by the RANS equations using the Spalart-Allmaras (SA) turbulence model [52] in the SA-neg form [3], expressed in terms of entropy variables [8]. We will consider two cases of uncertain parameters: uncertain flow conditions (with deterministic RANS-SA parameters); uncertain SA turbulence model parameters (with deterministic flow conditions). We again consider the three aforementioned refinement strategies: uniform refinement; isotropic adaptive  $h$ s refinement, which exploits spatio-stochastic structure but is suboptimal in exploiting the anisotropy in physical and stochastic spaces; and anisotropic adaptive  $h$ s refinement, which aims to fully exploit the anisotropic spatio-stochastic structure.

### 5.2.1. Case I: flow condition uncertainty quantification

We first consider a case with deterministic turbulence parameters and two uncertain flow conditions, namely we take the free stream Mach number  $M_\infty \sim \mathcal{U}[0.685, 0.715]$ , and the angle of attack  $\alpha \sim \mathcal{U}[2.20^\circ, 2.60^\circ]$ . The Reynolds number is fixed at  $\text{Re}_c = 6.5 \times 10^6$ . The quantity of interest is the mean drag on the airfoil. The SA turbulence model parameters are set to the default values [52]. The initial approximation space is given by the 506-element mesh provided for the AIAA High-Order Workshop [58], with quadratic polynomials in the physical space (i.e.,  $\{p^\kappa = 2\}_{\kappa \in \mathcal{T}_h}$ ), and linear polynomials in both stochastic dimensions (i.e.,  $\{s^\kappa = (1, 1)\}_{\kappa \in \mathcal{T}_h}$ ). The first component ( $k = 1$ ) of the mean ( $u_{h,p}^{(0,0)}$ ) and linear-linear ( $u_{h,p}^{(1,1)}$ ) mode strength are shown in Figure 7. The  $u_{h,p}^{(1,1)}$  mode strength shows that the shock will move towards the aft of the airfoil as both the Mach number and angle of attack are increased.

Figure 8a shows the relative error convergence of the uniform, isotropic adaptive, and anisotropic adaptive refinement schemes. The initial error is over 20% for the coarse spatio-stochastic space, which is unacceptable for practical aerodynamics simulations which seek  $\leq 1\%$  error. The error converges more rapidly for the anisotropic adaptation than the isotropic adaptation, which itself

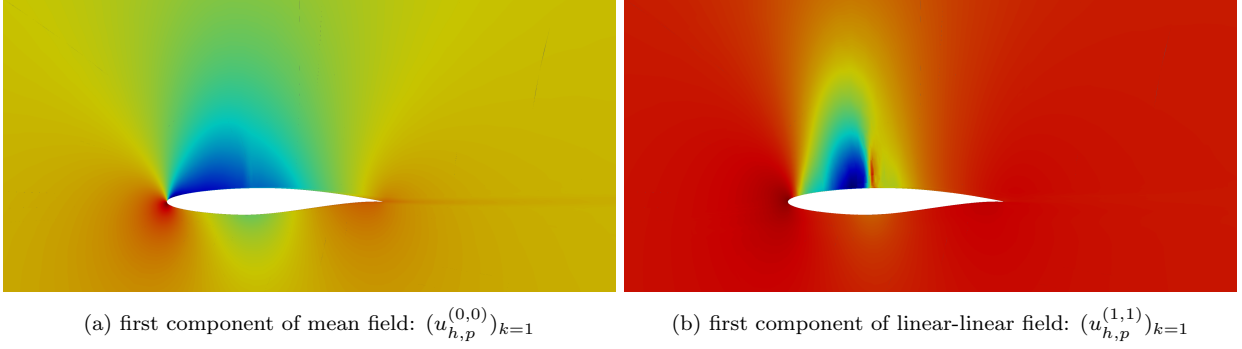


Figure 7: Examples of mode strengths for the transonic RANS-SA flow with uncertain flow conditions.

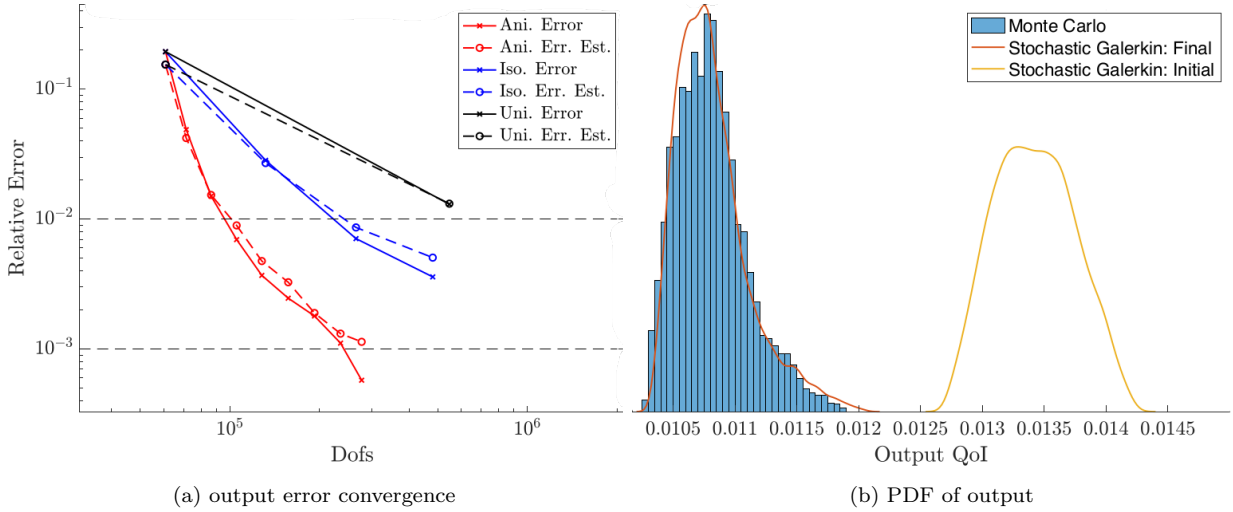


Figure 8: Left: output error convergence of the stochastic DG algorithms applied to the transonic RANS with uncertain flow conditions. Right: output distribution obtained using the anisotropic spatio-stochastic DG method in the first and final iterations as well as using Monte-Carlo method.

converges faster than the uniform refinement, as expected. We also note that the error estimates perform very well, with an effectivity close to unity for all cases. Figure 8b shows the drag distribution as computed by the anisotropic refinement scheme as well as the distribution computed with Monte Carlo with approximately 5000 samples of a deterministic anisotropic  $h$ -adaptive solution with a spatial error tolerance of  $10^{-6}$ . The final distributions are in good agreement. The initial distribution demonstrates the need for refinement in both the spatial and stochastic approximation spaces; linear polynomial chaos expansions on a coarse mesh fail to capture the errors resulting from the approximation of both the solution as well as the statistics of the solution. It is for this reason that reliable uncertainty quantification necessitates the combined control of both spatial and stochastic discretization error.

Figure 9 shows the approximation space  $\mathcal{V}_{h,p,s}$  obtained in the final anisotropic  $hs$  adaptation iteration. We observe that the adaptive method constructs very sparse fields as a result of the localized structure of the problem around the shock. The majority of the stochastic polynomial degrees are the order of the initial linear degree (i.e.,  $\{s^\kappa = (1, 1)\}_{\kappa \in \mathcal{T}_h}$ ), but up to fourth-order Mach number and fifth-order angle of attack expansions are used inside the shock. We also see the

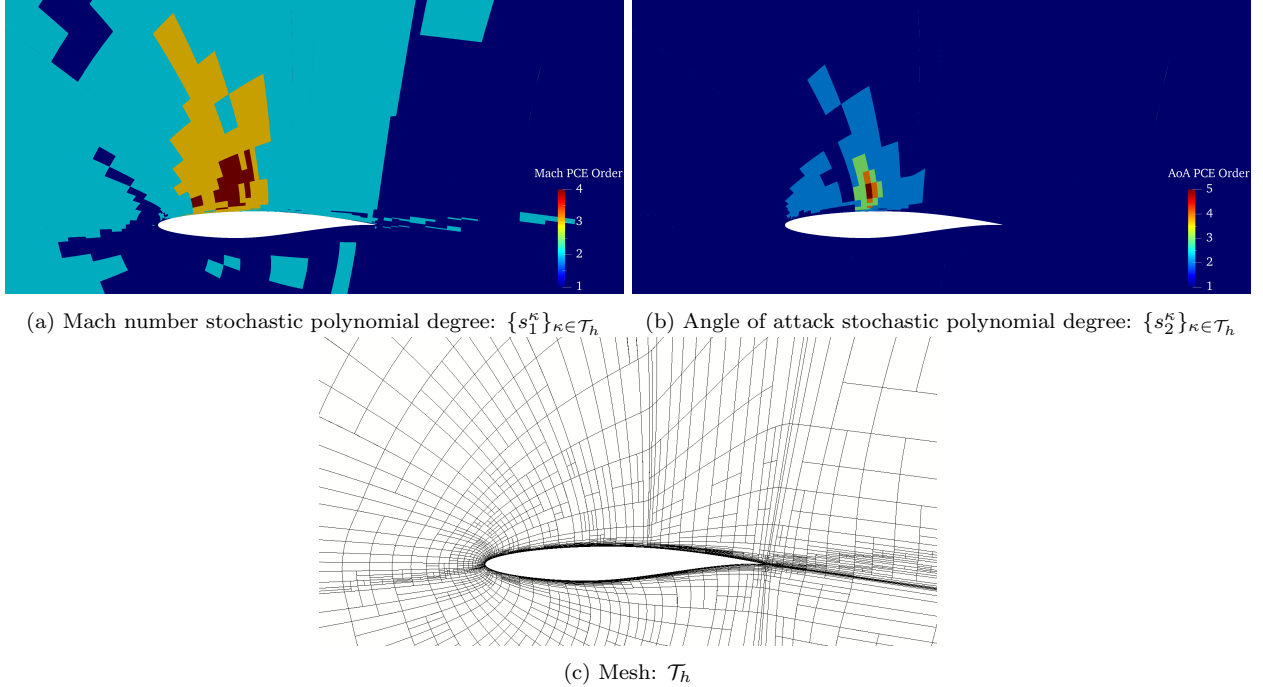


Figure 9: The approximation space  $\mathcal{V}_{h,p,s}$  generated by the anisotropic spatio-stochastic adaptive DG method for the RANS-SA problem with uncertain flow conditions.

exploitation of anisotropic structure in both the spatial and stochastic spaces: highly anisotropic elements are employed near the airfoil; quadratic stochastic polynomials are used over a wider area for the Mach number as compared with a more localized expansion for the angle of attack. We recall that each local PC mode strength is included only if they are deemed necessary by the local solver based on the behavior of the localized error estimate  $\{\eta_{\kappa_i}\}_{i=1}^{n_{\text{config}}}$ . This computational reduction is all accomplished in an automated fashion; the user needs to simply specify the flow condition and input distributions, and then the algorithm efficiently exploits the spatio-stochastic structure to provide reliable estimates for the quantity of interest without user intervention.

Table 2 shows a runtime breakdown for the spatio-stochastic adaptive DG methods and Monte Carlo method applied to the RANS problem to achieve an error of approximately 1%. Monte Carlo cumulative runtime was computed in the same manner as the advection-diffusion problem, with the equal error budget for the spatial and stochastic errors. The anisotropic and isotropic adaptation reach the target error level in the runtime equivalent of 8.1 and 28.8 Monte Carlo samples, respectively. The exploitation of the anisotropic localized spatio-stochastic structure leads to a runtime reduction of approximately 3.5 times relative to isotropic adaptation, which will increase further at a tighter error level. In fact the runtime for anisotropic adaptation is less than the runtime that would be required to collect 9 samples for a bi-quadratic non-intrusive polynomial chaos. While the uniform refinement algorithm does not reach a comparable error level, the primal solve for the second iteration takes the runtime equivalent of 19.4 Monte Carlo samples to obtain an error of approximately 10%. Furthermore, we note that for this more nonlinear and larger-scale problem, the local solves constitute a much smaller fraction of the overall runtime compared to the advection-diffusion case.

	primal solve	adjoint solve	local solves	cumulative
anisotropic adapt	1.07	0.58	0.20	8.1
isotropic adapt	21.89	6.80	-	28.8
Monte Carlo	0.12	0.01	-	133.2

Table 2: Runtime breakdown, normalized against the compute time for a single Monte Carlo sample, to reach the error of 1% for the RANS-SA problem with uncertain flow conditions. The first three columns shows the runtime for the final adaptation iteration — i.e., 4th and 3rd iteration for anisotropic and isotropic adaptation — only, and the last column shows the cumulative runtime for the entire adaptation process.

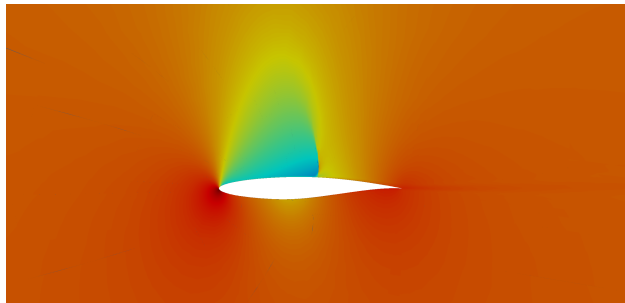


Figure 10: The first component of the mean field  $(u_{h,p}^{(0,0,0)})_{k=1}$  for the RANS-SA flow with uncertain turbulence model parameters.

### 5.2.2. Case II: Spalart-Allmaras turbulence model uncertainty quantification

We next consider an uncertainty quantification problem associated with the RANS-SA turbulence model. We choose for our uncertain variables the same SA turbulence parameters considered by Schaefer et al. [50]:  $\sigma \sim \mathcal{U}[0.60, 1.00]$ ,  $\kappa \sim \mathcal{U}[0.38, 0.42]$ , and  $c_{w3} \sim \mathcal{U}[1.75, 2.50]$ . The flow conditions are fixed:  $M_\infty = 0.729$ ,  $\text{Re} = 6.5 \times 10^6$ , and  $\alpha = 2.5478^\circ$ . The quantity of interest is the mean drag on the airfoil. The initial approximation space consists of 506 elements, quadratic polynomials in physical space (i.e.,  $\{p^\kappa = 2\}_{\kappa \in \mathcal{T}_h}$ ), and constant polynomials in stochastic space (i.e.,  $\{s^\kappa = (0, 0, 0)\}_{\kappa \in \mathcal{T}_h}$ ). Figure 10 shows the first component ( $k = 1$ ) of the mean field. This problem contrasts with the previous case with uncertainty in the flow conditions in that there is a significantly smaller effect from the input uncertainty with regard to the fact that the effects are both more localized and more linear.

Figure 11a shows relative error convergence of the isotropic adaptive and anisotropic adaptive refinement schemes. Uniform refinement is not performed as it is intractable for this  $d + P = 5$  dimensional problem; the number of degrees of freedom after a single step of uniform refinement is nearly  $5 \times 10^5$ . As the variations in the solution due to uncertainty in SA parameters is highly localized in the boundary layer and wake, there is ample opportunity to exploit the spatio-stochastic sparsity of the problem. Specifically, we see that in order to obtain an error of  $\approx 0.1\%$ , the anisotropic adaptation method requires a small fraction of what would be required for uniform refinement. We further note that exploiting the anisotropic structure in the stochastic parameter expansion significantly reduces the computational cost as compared with the isotropic case.

Figure 11b shows the drag distribution computed by the anisotropic adaptive stochastic DG method and the Monte Carlo method. We observe the key feature of our *goal-oriented* adaptive refinement; the algorithm recognizes that, in order to provide an accurate prediction of the mean, we need *not* provide an accurate estimate of the entire distribution. This focused, goal-oriented

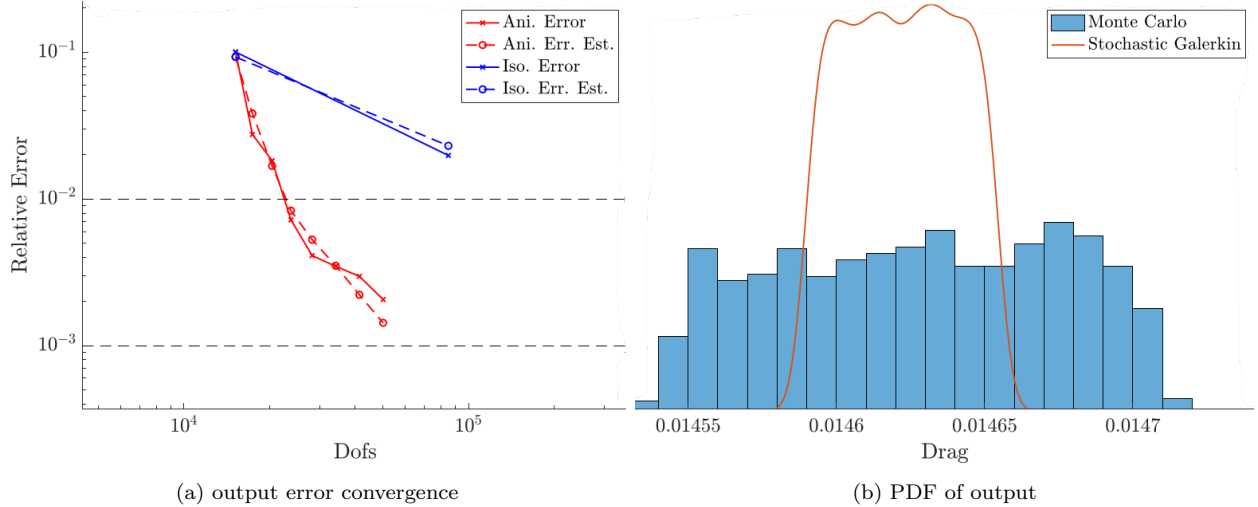


Figure 11: Left: output error convergence of the stochastic DG algorithms applied to the transonic RANS problem with uncertain turbulence model parameters. Right: output distribution obtained using the anisotropic spatio-stochastic DG method in the final iterations as well as using Monte-Carlo method.

adaptation allows the scheme to reduce the computational cost associated with the particular statistics (i.e., in the mean in this case) of the quantities of interest. In addition, the *a posteriori* error estimate allows us to be confident in the prediction even after such a focused adaptation that does not necessarily resolve the global spatio-stochastic behavior.

Figure 12 illustrates the approximation space  $\mathcal{V}_{h,p,s}$  resulting from the seventh and final anisotropic adaptation iteration. We see that in order to reach an error in the mean drag of  $\approx 0.1\%$  we require only linear PC expansions in the area of the spatial domain very close to the boundary layer of the airfoil; this is consistent with the fact that SA equation is only active in the boundary layer and wake. We also see that — just as was found by Schaefer et al. [50] — uncertainty in  $c_{w3}$  contributes little to the uncertainty in drag. The algorithm in fact has not selected to refine in this stochastic direction at all at the specified error level.

## Appendix A. Proof of output error bound

We now provide proofs for the approximation results presented in Section 3. All of the proofs are extensions of the results proven in [34] for the (space-only) DG method to the spatio-stochastic DG method.

*Proof of Proposition 3.* The result is an extension of Theorem 5.20 in [34] for deterministic DG spaces to spatio-stochastic DG spaces. We first prove (9). We note that  $\nabla(v - \Pi_{h,p,s}v) = \nabla(v - \Pi_s v) + \nabla(\Pi_s v - \Pi_{h,p,s}v)$  and hence

$$\|\nabla(v - \Pi_{h,p,s}v)\|_{L^2(\kappa \times \Xi)} \leq \|\nabla(v - \Pi_s v)\|_{L^2(\kappa \times \Xi)} + \|\nabla(\Pi_s v - \Pi_{h,p,s}v)\|_{L^2(\kappa \times \Xi)} \equiv \text{(I)} + \text{(II)}.$$

The term (I) is bounded by

$$\text{(I)}^2 = \|\nabla v - \Pi_s(\nabla v)\|_{L^2(\kappa \times \Xi)}^2 \leq \sum_{j=1}^P \frac{C}{(2s_j^\kappa)!(s_j^\kappa)! 2^{2(s_j^\kappa+1)}} \|\partial_{\xi_j}^{s_j^\kappa+1} \nabla v\|_{L^2(\kappa \times \Xi)}^2,$$

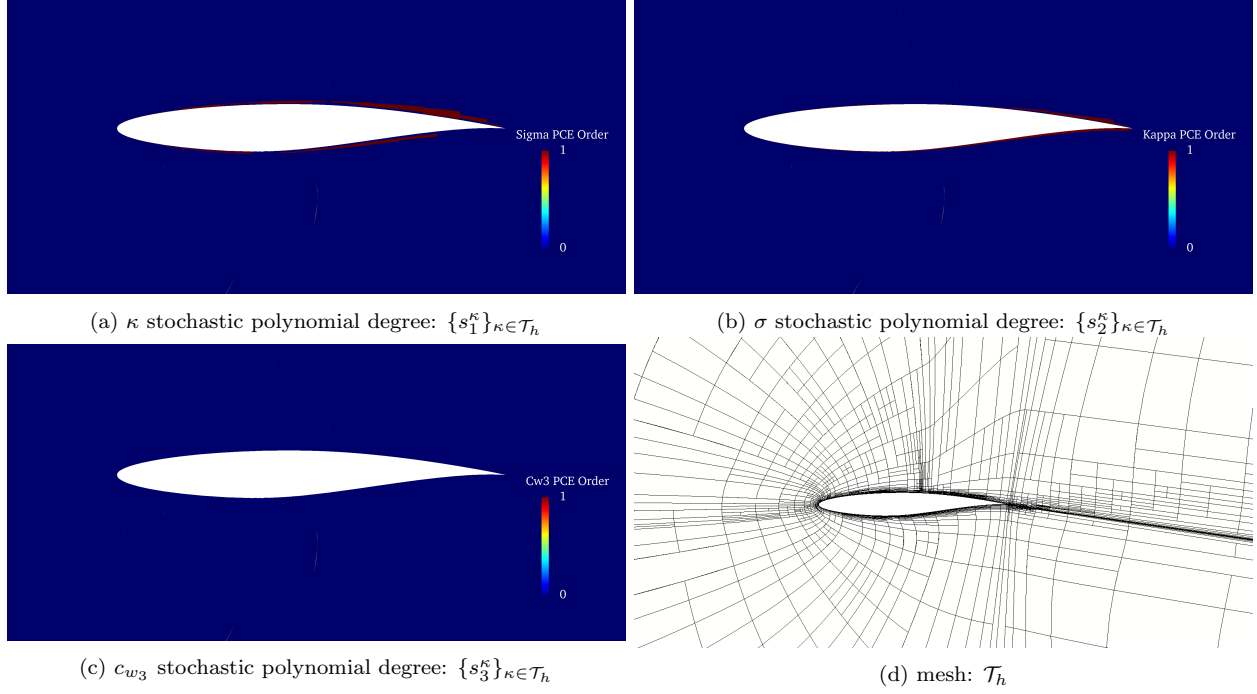


Figure 12: The approximation space  $\mathcal{V}_{h,p,s}$  generated by the anisotropic spatio-stochastic adaptive DG method for the RANS-SA problem with uncertain turbulence model parameters.

where the equality follows from the commutativity of physical-space derivative  $\nabla$  and stochastic-space projection  $\Pi_s$ , and the inequality follows from application of Lemma 6.9 of [34] to the function  $\nabla v$  in the  $d + P$ -dimensional space  $\kappa \times \Xi$ . We appeal to the definition of  $E_s^\kappa(\cdot)$  to obtain (I)  $\leq E_s^\kappa(\nabla v)$ .

We next observe that (II) simplifies to

$$(II) = \|\Pi_s(\nabla v - \nabla(\Pi_{h,p}v))\|_{L^2(\kappa \times \Xi)} \leq \|\nabla v - \nabla(\Pi_{h,p}v)\|_{L^2(\kappa \times \Xi)},$$

where the equality follows from  $\Pi_{h,p,s} = \Pi_s \Pi_{h,p}$  and the commutativity of  $\nabla$  and  $\Pi_s$ , and the inequality follows from the fact  $\Pi_s$  is the  $L^2$ -projection operator with the norm of unity. We hence obtain

$$\begin{aligned} \|\nabla v - \nabla(\Pi_{h,p}v)\|_{L^2(\kappa \times \Xi)}^2 &= \int_{\Xi} \|\nabla v(\cdot, \xi) - \nabla(\Pi_{h,p}v(\cdot, \xi))\|_{L^2(\kappa)}^2 d\mathbb{P}_\xi \\ &\leq \int_{\Xi} \int_{\kappa} \left( C |\sigma_{d,\kappa}|^{-k} D^{\kappa,p+1}(v(\cdot, \xi)) \right)^2 dx d\mathbb{P}_\xi, \end{aligned}$$

where the inequality follows from the first relationship of Theorem 5.20 of [34]. Straightforward simplification and the summation of (I) and (II) yield (9). The proof of (8) is analogous, except for the simplification due to the absence of the spatial derivative.

To prove (10), we again split the error into two parts:

$$\|v - \Pi_{h,p,s}v\|_{L^2(f \times \Xi)} = \|v - \Pi_s v\|_{L^2(f \times \Xi)} + \|\Pi_s v - \Pi_{h,p,s}v\|_{L^2(f \times \Xi)} \equiv (III) + (IV).$$

To bound (III), we again apply Lemma 6.9 of [34] to the function  $v|_f$  in the  $(d-1) + P$ -dimensional space  $f \times \Xi$ :

$$(III)^2 = \|v - \Pi_s v\|_{L^2(f \times \Xi)}^2 \leq \sum_{j=1}^P \frac{C}{(2s_j^\kappa)! (s_j^\kappa)^2 2^{2(s_j^\kappa+1)}} \|\partial_{\xi_j}^{s_j^\kappa+1} v\|_{L^2(f \times \Xi)}^2.$$

We then bound the term  $\|\partial_{\xi_j}^{s_j^\kappa+1} v\|_{L^2(f \times \Xi)}^2$  by trace inequality and scaling argument:

$$\|\partial_{\xi_j}^{s_j^\kappa+1} v\|_{L^2(f \times \Xi)}^2 \leq C \frac{|f|}{|\kappa|} \left( \|\partial_{\xi_j}^{s_j^\kappa+1} v\|_{L^2(\kappa \times \Xi)}^2 + (\sigma_1^\kappa)^2 \|\partial_{\xi_j}^{s_j^\kappa+1} \nabla v\|_{L^2(\kappa \times \Xi)}^2 \right).$$

We appeal to the definition of  $E_s^\kappa(\cdot)$  to obtain  $(III)^2 \leq \frac{|f|}{|\kappa|} (E_s^\kappa(v)^2 + (\sigma_1^\kappa)^2 E^\kappa(\nabla v)^2)$ . The bound of (IV) follows from the same argument as (II), except that we invoke the second relationship of Theorem 5.20 of [34] in the last step. The proof of (11) is analogous.  $\square$

Before we prove Proposition 7, we provide the following Lemma:

**Lemma 9.** *The error between the DG solution and best-fit projection  $\zeta \equiv \Pi_{h,p,s} u - u_{h,p,s}$  and the best-fit error  $\eta \equiv u - \Pi_{h,p,s}$  is related by*

$$\begin{aligned} \|\zeta\|_{\mathcal{V}_{h,p,s}}^2 &\leq C \sum_{\kappa \in \mathcal{T}_h} \left( \|\sqrt{a} \nabla \eta\|_{L^2(\kappa \times \Xi)}^2 + \gamma_1 \|\eta\|_{L^2(\kappa \times \Xi)}^2 + \|b \cdot n \eta^+\|_{L^2((\partial_+ \kappa \cap \Gamma) \times \Xi)}^2 \right. \\ &\quad \left. + \|b \cdot n \eta^-\|_{L^2((\partial_- \kappa \setminus \Gamma) \times \Xi)}^2 + \|\vartheta^{-1/2} \{a \nabla \eta\}\|_{L^2((\partial \kappa \setminus \Gamma_N) \times \Xi)}^2 + \|\vartheta^{1/2} \llbracket \eta \rrbracket\|_{L^2((\partial \kappa \setminus \Gamma_N) \times \Xi)}^2 \right), \end{aligned}$$

where  $\gamma_1|_\kappa = \|c/c_0\|_{L^\infty(\kappa \times \Xi)}^2$ , and  $C$  depends only on the dimension  $d$  and polynomial degree  $p$ .

*Proof.* The proof is a straightforward extension of the proof of Lemma 5.22 in [34] to the stochastic DG method. We first note that by coercivity and Galerkin orthogonality  $\alpha \|\zeta\|_{\mathcal{V}_{h,p,s}}^2 \leq |\mathcal{B}_{h,p,s}(\zeta, \zeta)| = |\mathcal{B}_{h,p,s}(\eta, \zeta)|$ . Tedious but straightforward manipulations under the aforementioned assumption  $b \cdot \nabla v \in \mathcal{V}_{h,p,s} \forall v \in \mathcal{V}_{h,p,s}$  yields the desired result.  $\square$

*Proof of Proposition 7.* The proof is an extension of Theorem 5.23 in [34] to the stochastic DG method. By the definition of the adjoint  $z$  and Galerkin orthogonality we obtain

$$\begin{aligned} \mathcal{J}(u) - \mathcal{J}_{h,p,s}(u_{h,p,s}) &= \mathcal{B}_{h,p,s}(u - u_{h,p,s}, z - \Pi_{h,p,s} z) \\ &= \mathcal{B}_{h,p,s}(u - \Pi_{h,p,s} u, z - \Pi_{h,p,s} z) + \mathcal{B}_{h,p,s}(\Pi_{h,p,s} u - u_{h,p,s}, z - \Pi_{h,p,s} z) \\ &= \mathcal{B}_{h,p,s}(\eta, w) + \mathcal{B}_{h,p,s}(\zeta, w) = (I) + (II), \end{aligned}$$

where  $\eta \equiv u - \Pi_{h,p,s} u$ ,  $\zeta \equiv \Pi_{h,p,s} u - u_{h,p,s}$ , and  $w \equiv z - \Pi_{h,p,s} z$ . By a straightforward extension of the manipulation in [34] to the stochastic DG method that appeals to  $\mathcal{B}(w, v) \equiv$

$\int_{\xi} \mathcal{B}(w(\cdot, \xi), v(\cdot, \xi); \xi) d\mathbb{P}_{\xi}$ , we obtain

$$\begin{aligned}
(\text{I}) &\leq C \left( \sum_{\kappa \in \mathcal{T}_h} \left( \|\sqrt{a} \nabla \eta\|_{L^2(\kappa \times \Xi)}^2 + \beta_1 \|\eta\|_{L^2(\kappa \times \Xi)}^2 + \beta_2 \epsilon_{\kappa}^{-1} \|\nabla \eta\|_{L^2(\kappa \times \Xi)}^2 + \beta_2 \|\llbracket \eta \rrbracket\|_{L^2(\partial_{-\kappa} \times \Xi)}^2 \right. \right. \\
&\quad \left. \left. + \|\vartheta^{-1/2} \{a \nabla \eta\}\|_{L^2((\partial \kappa \cap \Gamma_N) \times \Xi)} + \|\vartheta^{1/2} \llbracket \eta \rrbracket\|_{L^2((\partial \kappa \setminus \Gamma_N) \times \Xi)}^2 \right) \right) \\
&\times \left( \sum_{\kappa \in \mathcal{T}_h} \left( \|\sqrt{a} \nabla w\|_{L^2(\kappa \times \Xi)}^2 + (\beta_1 + \beta_2 \epsilon_{\kappa}) \|w\|_{L^2(\kappa \times \Xi)}^2 + \beta_2 \|w^+\|_{L^2(\partial_{-\kappa} \times \Xi)}^2 \right. \right. \\
&\quad \left. \left. + \|\vartheta^{-1/2} \{a \nabla w\}\|_{L^2((\partial \kappa \setminus \Gamma_N) \times \Xi)} + \|\vartheta^{1/2} \llbracket w \rrbracket\|_{L^2((\partial \kappa \setminus \Gamma_N) \times \Xi)}^2 \right) \right).
\end{aligned}$$

A similar extension of the manipulation in [34] yields

$$\begin{aligned}
(\text{II}) = |\mathcal{B}(\zeta, w)| &\leq \|\zeta\|_{\mathcal{V}_{h,p,s}} \left( \sum_{\kappa \in \mathcal{T}_h} \left( \|\sqrt{a} \nabla w\|_{L^2(\kappa \times \Xi)}^2 + \gamma_2 \|w\|_{L^2(\kappa \times \Xi)}^2 + \beta_2 \|w^+\|_{L^2(\partial_{-\kappa} \times \Xi)}^2 \right. \right. \\
&\quad \left. \left. + \|\vartheta^{1/2} \llbracket w \rrbracket\|_{L^2((\partial \kappa \setminus \Gamma_N) \times \Xi)}^2 + \|\vartheta^{-1/2} \{a \nabla w\}\|_{L^2((\partial \kappa \setminus \Gamma_N) \times \Xi)}^2 \right) \right)^{1/2}.
\end{aligned}$$

We invoke Lemma 9 on  $\|\zeta\|_{\mathcal{V}_{h,p,s}}$  and sum (I) and (II) to obtain

$$|\mathcal{J}(u) - \mathcal{J}_{h,p,s}(u_{h,p,s})|^2 \leq C \sum_{\kappa \in \mathcal{T}_h} (\tilde{e}_{\text{pr}}^{\kappa}) \sum_{\kappa \in \mathcal{T}_h} (\tilde{e}_{\text{du}}^{\kappa}),$$

where

$$\begin{aligned}
\tilde{e}_{\text{pr}}^{\kappa} &= \|\sqrt{a} \nabla \eta\|_{L^2(\kappa \times \Xi)}^2 + (\beta_1 + \gamma_1) \|\eta\|_{L^2(\kappa \times \Xi)}^2 + \beta_2 \epsilon_{\kappa}^{-1} \|\nabla \eta\|_{L^2(\kappa \times \Xi)}^2 \\
&\quad + \beta_2 \|\eta^+\|_{L^2((\partial_+ \kappa \cap \Gamma) \times \Xi)}^2 + \beta_2 \|\eta^-\|_{L^2((\partial_{-\kappa} \setminus \Gamma) \times \Xi)}^2 + \beta_2 \|\llbracket \eta \rrbracket\|_{L^2(\partial_{-\kappa} \times \Xi)}^2 \\
&\quad + \|\vartheta^{-1/2} \{a \nabla \eta\}\|_{L^2((\partial \kappa \setminus \Gamma_N) \times \Xi)} + \|\vartheta^{1/2} \llbracket \eta \rrbracket\|_{L^2((\partial \kappa \setminus \Gamma_N) \times \Xi)}^2 \\
\tilde{e}_{\text{du}}^{\kappa} &= \|\sqrt{a} \nabla w\|_{L^2(\kappa \times \Xi)}^2 + (\beta_1 + \beta_2 \epsilon_{\kappa} + \gamma_2) \|w\|_{L^2(\kappa \times \Xi)}^2 + \beta_2 \|w^+\|_{L^2(\partial_{-\kappa} \times \Xi)}^2 \\
&\quad + \|\vartheta^{-1/2} \{a \nabla w\}\|_{L^2((\partial \kappa \setminus \Gamma_N) \times \Xi)} + \|\vartheta^{1/2} \llbracket w \rrbracket\|_{L^2((\partial \kappa \setminus \Gamma_N) \times \Xi)}^2.
\end{aligned}$$

We now invoke the projection error bounds in Proposition 3, set the stabilization parameter to  $\vartheta = Ca \frac{|f|}{|\kappa|}$ , choose  $\epsilon = (\sigma_d^{\kappa})^{-1}$ , and note  $\frac{|f|}{|\kappa|} \leq (\sigma_d^{\kappa})^{-1}$ . Tedious but straightforward manipulations yield the desired result.  $\square$

## Acknowledgment

The financial support for this work was provided by the Natural Sciences and Engineering Research Council of Canada and the Kenneth M Molson Foundation. Some of the computations were performed on the Niagara supercomputer at the SciNet HPC Consortium. SciNet is funded by the Canada Foundation for Innovation; the Government of Ontario; Ontario Research Fund - Research Excellence; and the University of Toronto. We would also like to thank anonymous reviewers for very helpful feedback that has improved this manuscript.

## References

- [1] R. Abgrall and S. Mishra. Uncertainty quantification for hyperbolic systems of conservation laws. In *Handbook of Numerical Analysis*, volume 18, pages 507–544. Elsevier, 2017.
- [2] M. Ainsworth and J. T. Oden. A posteriori error estimation in finite element analysis. *Computer Methods in Applied Mechanics and Engineering*, 142:1–88, 1997.
- [3] S. R. Allmaras, F. T. Johnson, and P. R. Spalart. Modifications and clarifications for the implementation of the Spalart-Allmaras turbulence model. 7th International Conference on Computational Fluid Dynamics ICCFD7-1902, ICCFD, 2012.
- [4] R. C. Almeida and J. T. Oden. Solution verification, goal-oriented adaptive methods for stochastic advection-diffusion problems. *Computer Methods in Applied Mechanics and Engineering*, 199(37-40):2472–2486, August 2010.
- [5] D. N. Arnold, F. Brezzi, B. Cockburn, and L. D. Marini. Unified analysis of discontinuous Galerkin methods for elliptical problems. *SIAM Journal on Numerical Analysis*, 39(5):1749–1779, 2002.
- [6] I. Babuška, F. Nobile, and R. Tempone. A stochastic collocation method for elliptic partial differential equations with random input data. *SIAM Journal on Numerical Analysis*, 45(3):1005–1034, 2007.
- [7] I. Babuska, R. Tempone, and G. E. Zouraris. Galerkin finite element approximations of stochastic elliptic partial differential equations. *SIAM Journal on Numerical Analysis*, 42(2):800–825, 2004.
- [8] T. J. Barth. Numerical methods for gasdynamic systems on unstructured meshes. In D. Kröner, M. Ohlberger, and C. Rohde, editors, *An Introduction to Recent Developments in Theory and Numerics for Conservation Laws*, pages 195–282. Springer-Verlag, 1999.
- [9] T. J. Barth. Simplified discontinuous Galerkin methods for systems of conservation laws with convex extension. NAS Technical Report NAS-99-009, NASA, 1999.
- [10] T. J. Barth. An overview of combined uncertainty and a posteriori error bound estimates for CFD calculations. AIAA 2016-1062, AIAA, 2016.
- [11] F. Bassi and S. Rebay. GMRES discontinuous Galerkin solution of the compressible Navier-Stokes equations. In B. Cockburn, G. E. Karniadakis, and C.-W. Shu, editors, *Discontinuous Galerkin Methods: Theory, Computation and Applications*, pages 197–208. Springer, Berlin, 2000.
- [12] R. Becker and R. Rannacher. An optimal control approach to a posteriori error estimation in finite element methods. *Acta Numerica*, 10:1–102, May 2001.
- [13] A. Bepalov, D. Praetorius, L. Rocchi, and M. Ruggeri. Goal-oriented error estimation and adaptivity for elliptic PDEs with parametric or uncertain inputs. *Computer Methods in Applied Mechanics and Engineering*, 345:951–982, 2019.

- [14] A. Bourlioux, A. Ern, and P. Turbis. A posteriori error estimation for subgrid flamelet models. *Multiscale Modeling and Simulation*, 8(2):481–497, Jan 2010.
- [15] C. Bryant, S. Prudhomme, and T. Wildey. Error decomposition and adaptivity for response surface approximations from PDEs with parametric uncertainty. *SIAM/ASA Journal on Uncertainty Quantification*, 3(1):1020–1045, 2015.
- [16] T. Butler, C. Dawson, and T. Wildey. A posteriori error analysis of stochastic differential equations using polynomial chaos expansions. *SIAM Journal on Scientific Computing*, 33(3):1267–1291, 2011.
- [17] M. Ceze and K. J. Fidkowski. Anisotropic hp-adaptation framework for functional prediction. *AIAA Journal*, 51(2):492–509, 2012.
- [18] B. Cockburn. Discontinuous Galerkin methods. *ZAMM-Journal of Applied Mathematics and Mechanics/Zeitschrift für Angewandte Mathematik und Mechanik*, 83(11):731–754, 2003.
- [19] B. J. Deusschere, H. N. Najm, P. P. Pébay, O. M. Knio, R. G. Ghanem, and O. P. L. Maitre. Numerical challenges in the use of polynomial chaos representations for stochastic processes. *SIAM Journal on Scientific Computing*, 26(2):698–719, Jan 2004.
- [20] E. Dow and Q. Wang. Uncertainty quantification of structural uncertainties in RANS simulations of complex flows. In *20th AIAA Computational Fluid Dynamics Conference*, page 3865, 2011.
- [21] M. Eigel, C. J. Gittelsohn, C. Schwab, and E. Zander. Adaptive stochastic Galerkin FEM. *Comput. Methods Appl. Mech. Engrg.*, 270:247–269, 2013.
- [22] M. Eigel, C. J. Gittelsohn, C. Schwab, and E. Zander. A convergent adaptive stochastic galerkin finite element method with quasi-optimal spatial meshes. *ESAIM: Mathematical Modelling and Numerical Analysis*, 49(5):1367–1398, Aug 2015.
- [23] M. Eigel, M. Pfeffer, and R. Schneider. Adaptive stochastic Galerkin FEM with hierarchical tensor representations. *Numerische Mathematik*, 136(3):765–803, 2017.
- [24] K. Fidkowski and D. Darmofal. Review of output-based error estimation and mesh adaptation in computational fluid dynamics. *AIAA Journal*, 49(4):673–694, 2011.
- [25] E. H. Georgoulis, E. Hall, and P. Houston. Discontinuous Galerkin methods for advection-diffusion-reaction problems on anisotropically refined meshes. *SIAM Journal on Scientific Computing*, 30(1):246–271, Jan 2007.
- [26] E. H. Georgoulis, E. Hall, and P. Houston. Discontinuous Galerkin methods on hp-anisotropic meshes I: a priori error analysis. *International Journal of Computing Science and Mathematics*, 1(2-4):221–244, 2007.
- [27] E. H. Georgoulis, E. Hall, and P. Houston. Discontinuous Galerkin methods on hp-anisotropic meshes II: a posteriori error analysis and adaptivity. *Applied Numerical Mathematics*, 59(9):2179–2194, Sep 2009.

- [28] R. Ghanem and P. D. Spanos. Polynomial chaos in stochastic finite elements. *Journal of Applied Mechanics*, 57(1):197–202, 1990.
- [29] M. Giles, N. Pierce, M. Giles, and N. Pierce. Adjoint equations in CFD - duality, boundary conditions and solution behaviour. In *13th Computational Fluid Dynamics Conference*. American Institute of Aeronautics and Astronautics, Jun 1997.
- [30] M. B. Giles. Multilevel Monte Carlo path simulation. *Operations Research*, 56(3):607–617, 2008.
- [31] D. Guignard and F. Nobile. A posteriori error estimation for the stochastic collocation finite element method. *SIAM Journal on Numerical Analysis*, 56(5):3121–3143, 2018.
- [32] D. Guignard, F. Nobile, and M. Picasso. A posteriori error estimation for elliptic partial differential equations with small uncertainties. *Numerical Methods for Partial Differential Equations*, 32(1):175–212, Aug 2015.
- [33] R. Hartmann. Adjoint consistency analysis of discontinuous Galerkin discretizations. *SIAM Journal on Numerical Analysis*, 45(6):2671–2696, 2007.
- [34] R. Hartmann and P. Houston. Error estimation and adaptive mesh refinement for aerodynamic flows. In H. Deconinck, editor, *VKI LS 2010-01: 36<sup>th</sup> CFD/ADIGMA course on hp-adaptive and hp-multigrid methods, Oct. 26-30, 2009*. Von Karman Institute for Fluid Dynamics, Rhode Saint Genèse, Belgium, 2009.
- [35] J. S. Hesthaven and T. Warburton. *Nodal discontinuous Galerkin methods*. Springer New York, 2008.
- [36] P. Houston, C. Schwab, and E. Süli. Discontinuous *hp*-finite element methods for advection-diffusion-reaction problems. *SIAM Journal on Numerical Analysis*, 39(6):2133–2163, Jan 2002.
- [37] O. M. Knio and O. L. Maitre. Uncertainty propagation in CFD using polynomial chaos decomposition. *Fluid dynamics research*, 38(9):616, 2006.
- [38] O. L. Maitre and O. M. Knio. *Spectral methods for uncertainty quantification*. Springer, 2010.
- [39] L. Mathelin and O. L. Maître. Dual-based a posteriori error estimate for stochastic finite element methods. *Communications in Applied Mathematics and Computational Science*, 2(1):83–115, Sep 2007.
- [40] H. N. Najm. Uncertainty quantification and polynomial chaos techniques in computational fluid dynamics. *Annual Review of Fluid Mechanics*, 41:35–52, 2009.
- [41] W. L. Oberkampf, T. G. Trucano, and C. Hirsch. Verification, validation, and predictive capability in computational engineering and physics. *Applied Mechanics Reviews*, 57(5):345–384, Sep 2004.
- [42] J. Oden and S. Prudhomme. Goal-oriented error estimation and adaptivity for the finite element method. *Computers & Mathematics with Applications*, 41(5-6):735–756, Mar 2001.

- [43] J. Oden and S. Prudhomme. Estimation of modeling error in computational mechanics. *Journal of Computational Physics*, 182(2):496–515, Nov 2002.
- [44] J. Oden and K. S. Vemaganti. Estimation of local modeling error and goal-oriented adaptive modeling of heterogeneous materials: Part I. error estimates and adaptive algorithms. *Journal of Computational Physics*, 164(1):22–47, Oct 2000.
- [45] T. A. Oliver and D. L. Darmofal. Analysis of dual consistency for discontinuous Galerkin discretizations of source terms. *SIAM Journal on Numerical Analysis*, 47(5):3507–3525, 2009.
- [46] P.-O. Persson and J. Peraire. Newton-GMRES preconditioning for discontinuous Galerkin discretizations of the Navier-Stokes equations. *SIAM Journal on Scientific Computing*, 30(6):2709–2733, Jan 2008.
- [47] D. A. D. Pietro and A. Ern. *Mathematical aspects of discontinuous Galerkin methods*. Springer Berlin Heidelberg, 2012.
- [48] S. Prudhomme and J. T. Oden. Computable error estimators and adaptive techniques for fluid flow problems. In *Error Estimation and Adaptive Discretization Methods in Computational Fluid Dynamics*, pages 207–268. Springer Berlin Heidelberg, 2003.
- [49] Y. Saad and M. H. Schultz. GMRES: a generalized minimal residual algorithm for solving nonsymmetric linear systems. *SIAM Journal on scientific and statistical computing*, 7(3):856–869, 1986.
- [50] J. Schaefer, A. Cary, M. Mani, and P. Spalart. Uncertainty quantification and sensitivity analysis of SA turbulence model coefficients in two and three dimensions. AIAA 2017-1710, AIAA, 2017.
- [51] J. Slotnick, A. Khodadoust, J. Alonso, D. Darmofal, W. Gropp, E. Lurie, and D. Mavriplis. CFD vision 2030 study: a path to revolutionary computational aerosciences. Nasa/cr-2014-218178, NASA, 2014.
- [52] P. R. Spalart and S. R. Allmaras. A one-equation turbulence model for aerodynamics flows. *La Recherche Aéronautique*, 1:5–21, 1994.
- [53] J. Van Langenhove, D. Lucor, F. Alauzet, and A. Belme. Goal-oriented error control of stochastic system approximations using metric-based anisotropic adaptations. *Journal of Computational Physics*, 374:384–412, 2018.
- [54] K. S. Vemaganti and J. Oden. Estimation of local modeling error and goal-oriented adaptive modeling of heterogeneous materials: Part II: a computational environment for adaptive modeling of heterogeneous elastic solids. *Computer Methods in Applied Mechanics and Engineering*, 190(46-47):6089–6124, Sep 2001.
- [55] X. Wan and G. Karniadakis. Error control in multi-element generalized polynomial chaos method for elliptic problems with random coefficients. *Communications in Computational Physics*, 5:793–820, 03 2009.

- [56] X. Wan and G. E. Karniadakis. An adaptive multi-element generalized polynomial chaos method for stochastic differential equations. *Journal of Computational Physics*, 209(2):617–642, 2005.
- [57] X. Wan and G. E. Karniadakis. Multi-element generalized polynomial chaos for arbitrary probability measures. *SIAM Journal on Scientific Computing*, 28(3):901–928, 2006.
- [58] Z. J. Wang, K. Fidkowski, R. Abgrall, F. Bassi, D. Caraeni, A. Cary, H. Deconinck, R. Hartmann, K. Hillewaert, H. T. Huynh, N. Kroll, G. May, P.-O. Persson, B. van Leer, and M. Visbal. High-order CFD methods: current status and perspective. *International Journal for Numerical Methods in Fluids*, 72(8):811–845, 2013.
- [59] N. Wiener. The homogeneous chaos. *American Journal of Mathematics*, 60(4):897–936, 1938.
- [60] H. Xiao and P. Cinnella. Quantification of model uncertainty in RANS simulations: a review. *Progress in Aerospace Sciences*, 108:1–31, Jul 2019.
- [61] D. Xiu and J. S. Hesthaven. High-order collocation methods for differential equations with random inputs. *SIAM Journal on Scientific Computing*, 27(3):1118–1139, 2005.
- [62] M. Yano and D. L. Darmofal. An optimization-based framework for anisotropic simplex mesh adaptation. *Journal of Computational Physics*, 231(22):7626–7649, 2012.
- [63] M. Yano, J. M. Modisette, and D. Darmofal. The importance of mesh adaptation for higher-order discretizations of aerodynamic flows. AIAA 2011-3852, AIAA, 2011.